



H63D HFE genotype accelerates disease progression in animal models of amyotrophic lateral sclerosis



Wint Nandar^a, Elizabeth B. Neely^a, Zachary Simmons^b, James R. Connor^{a,*}

^a Department of Neurosurgery, The Pennsylvania State University, M. S. Hershey Medical Center, Hershey, PA 17033, USA

^b Department of Neurology, The Pennsylvania State University, M. S. Hershey Medical Center, Hershey, PA 17033, USA

ARTICLE INFO

Article history:

Received 1 June 2014

Received in revised form 3 September 2014

Accepted 29 September 2014

Available online 5 October 2014

Keywords:

H63D HFE

SOD1(G93A)

ALS

Iron

Oxidative stress

Gliosis

ABSTRACT

H63D HFE is associated with iron dyshomeostasis and oxidative stress; each of which plays an important role in amyotrophic lateral sclerosis (ALS) pathogenesis. To examine the role of H63D HFE in ALS, we generated a double transgenic mouse line (SOD1/H67D) carrying the H67D HFE (homologue of human H63D) and SOD1(G93A) mutations. We found double transgenic mice have shorter survival and accelerated disease progression. We examined parameters in the lumbar spinal cord of double transgenic mice at 90 days (presymptomatic), 110 days (symptomatic) and end-stage. Transferrin receptor and L-ferritin expression, both indicators of iron status, were altered in double transgenic and SOD1 mice starting at 90 days, indicating loss of iron homeostasis in these mice. However, double transgenic mice had higher L-ferritin expression than SOD1 mice. Double transgenic mice exhibited increased Iba-1 immunoreactivity and caspase-3 levels, indicating increased microglial activation which would be consistent with the higher L-ferritin levels. Although both SOD1 and double transgenic mice had increased GFAP expression, the magnitude of the increase was higher in double transgenic mice at 110 days, suggesting increased gliosis in these mice. Increased hemoxygenase-1 and decreased nuclear factor E2-related factor 2 levels in double transgenic mice strongly suggest the accelerated disease process could be associated with increased oxidative stress. There was no evidence of TAR-DNA-binding protein 43 mislocalization to the cytoplasm in double transgenic mice; however, there was evidence suggesting neurofilament disruption, which has been reported in ALS. Our findings indicate H63D HFE modifies ALS pathophysiology via pathways involving oxidative stress, gliosis and disruption of cellular functions.

© 2014 Elsevier B.V. All rights reserved.

1. Introduction

Amyotrophic lateral sclerosis (ALS), commonly known as Lou Gehrig's disease, is characterized by degeneration of lower and upper motor neurons in the brainstem, spinal cord, and the motor cortex. The worldwide incidence of ALS is 1–2 per 100,000 and the average age of clinical onset is 55–60 years with an average survival of 3 to 5 years after symptom onset [1,2]. However, the range of survival is from a few months to more than a decade after onset [3]. Because of the high variability in age of onset and in survival, ALS is proposed to be a heterogeneous disease. The majority of ALS cases (90–95%) are sporadic (SALS), whereas 5–10% are inherited (familial ALS, or FALS). Despite identification of mutations in a number of genes associated with FALS and SALS [1,2] including superoxide dismutase (SOD; [4]),

TAR-DNA-binding protein 43 (TDP 43; [5]), fused in sarcoma/translated in liposarcoma (FUS/TLS; [6]) and chromosome 9 open reading frame 72 (C9ORF72; [7]), the etiology in most patients with ALS remains inconclusive, and the molecular mechanisms contributing to motor neuron degeneration in ALS have not been elucidated.

Loss of iron homeostasis and the associated oxidative stress are significant parts of the disease processes in neurodegenerative diseases including ALS [8]. Higher iron levels in the central nervous system [9,10] and elevated serum ferritin have been reported in ALS patients [11–13]. Treatment with iron chelators delayed onset, extended survival and prevented motor neuron degeneration in ALS mouse models [14,15]. These reports suggest an important role of iron metabolism in ALS pathogenesis. Therefore, we began studies to determine if there were polymorphisms associated with iron metabolism that could influence the ALS phenotype.

One of the genes involved in iron homeostasis is the HFE gene. Two common HFE polymorphisms are H63D and C282Y with worldwide allelic frequencies of 8.1% and 1.9% respectively. The C282Y HFE polymorphism is mostly associated with hereditary hemochromatosis (HH), the most common iron overload genetic disorder in Caucasian population (1/200). The occurrence of the H63D HFE in HH is lower than C282Y [16]. However, increasing evidence suggests an association

Abbreviations: GSH, glutathione; HH, hemochromatosis; HO-1, hemoxygenase-1; NFH, heavy-chain neurofilament protein; Nrf2, nuclear factor E2-related factor 2; SOD, superoxide dismutase; TDP-43, TAR DNA-binding protein 43; TfR, transferrin receptor

* Corresponding author at: Department of Neurosurgery, The Pennsylvania State University, College of Medicine, 500 University Drive (H110), Hershey, PA 17033-0850, USA. Tel.: +1 717 531 4541; fax: +1 717 531 0091.

E-mail addresses: wnandar@hmc.psu.edu (W. Nandar), eneely@psu.edu (E.B. Neely), zsimmmons@hmc.psu.edu (Z. Simmons), jconnor@psu.edu (J.R. Connor).

of H63D HFE with neurodegenerative diseases including ALS [17]. Five independent groups in the United States [18], the United Kingdom [19], Italy [20], the Netherlands [21] and China [22] have reported a positive association between H63D HFE and ALS. Although three studies [23–25] reported no association between H63D HFE and ALS, in all studies, there is agreement that H63D HFE is present in as many as 30% of ALS patients [18–21,23–25]. Moreover, a meta-analysis indicates that the presence of the H63D HFE variant increases the risk of developing ALS by 4-fold [26].

The existing paradigm regarding HFE gene variants and brain function holds that the brain is protected from iron accumulation associated with the HFE polymorphisms because of the blood-brain-barrier. Recent MRI studies, however, suggest that people with HFE polymorphisms have more brain iron and increased cognitive impairment with age [27–30]. In an animal model, the presence of H67D HFE (homologous to H63D in human) disrupts brain iron homeostasis and is associated with increased oxidative stress in the brain [31] and significant disruptions in cholesterol metabolism [32]. The alterations in iron homeostasis and increased oxidative stress are also seen at the cellular level [33], along with increased glutamate release [34] and increased endoplasmic reticulum (ER) stress [35]. Each of above mechanisms is considered a contributing factor to ALS pathogenesis [1,36]. Thus, the data strongly argue that H63D HFE is a genetic modifier for the risk of ALS, and warrant the development of an animal model as presented herein.

Based on findings from our previous *in vitro* and *in vivo* studies, we hypothesized that H63D HFE increases the risk of ALS by establishing a permissive milieu that promotes the convergence of disease mechanisms in ALS. To directly test our hypothesis, we generated a double transgenic mouse line (SOD1/H67D) that carries both H67D HFE (homologous to H63D in humans) and SOD1(G93A) mutations. We found that H63D HFE shortens survival and disease duration in double transgenic mice. Elevated oxidative stress, microglial toxicity and dysregulation of iron homeostasis contribute to an accelerated disease in these mice. Given the data that indicate 1/3 of patients with ALS carry the H63D gene variant, the double transgenic mouse model could serve as a critical preclinical model to evaluate how the H63D HFE genotype can impact the disease process and treatment strategies for ALS patients.

2. Materials and methods

2.1. Generation of double transgenic mice (SOD1/H67D)

SOD1(G93A) male mice (strain name: B6SJL-Tg(SOD1-G93A)1Gur/J; #002726) purchased from Jackson Labs (Bar Harbor, ME) were crossbred with H67D/H67D (homologue of human H63D) or wild-type HFE female mice (strain name: B6;129X1-Hfe^{tm1Jrc0}/J) to generate a double transgenic mouse line, that carries H67D HFE as well as SOD1(G93A) mutation. The H67D colony is maintained at Penn State Hershey Medical Center. Cohorts used for crossbreeding were chosen from littermates. SOD1(G93A) and wild-type (WT) mice from the same litters as the double transgenic mice were included in all experiments. Both males and females were included in all experiments.

Animals were maintained under normal housing conditions with *ad libitum* access to food and water. All experiments were performed according to the NIH Guide for the Care and Use of Laboratory Animals and were approved by the Pennsylvania State University College of Medicine Institutional Animal Care and Use Committee.

2.2. Genotyping

The H67D HFE genotyping was performed as previously reported [31]. Briefly, DNA was extracted from tail biopsies using DNeasy blood and tissue kit (QIAGEN, Valencia, CA). PCR was

performed using following forward and reverse primers: (5' AGGACTCACTCTCTGGCAGCAGGAGGTAACCA3') and (5' TTTCTTTTACAAAGCTATATCCCCAGGGT3'). Following PCR, DNA was digested with *Bsp*HI restriction enzyme for 2 hours at 37 °C to detect H67D point mutation. The PCR product was separated by 1.5% agarose gel electrophoresis. DNA from WT mice digested by *Bsp*HI resulted 240 and 260 bp and DNA from wt/H67D mice resulted 500, 240 and 260 bp. Genotyping for SOD1(G93A) mutation was performed using primers that specifically amplifying a 236-bp DNA fragment carrying a G93A mutation. The forward and reverse primers are: 5'CATCAGCCCTAATCCATCTGA-3' and 5'-CGCGACTAACAATCAAAGTGA-3'. PCR conditions for SOD1(G93A) genotyping are 95 °C for 3 minutes, 95 °C for 30 s, 60 °C for 30 s, 35 cycles of 72 °C for 45 s and 72 °C for 2 min.

The SOD1/H67D mice are heterozygous for H67D HFE and also carry G93A mutation while SOD1(G93A) mice carry wild-type HFE and G93A mutation (data not shown).

2.3. Behavior and survival

2.3.1. Rotarod

Starting at 49 days of age, motor performance was tested on a rotarod apparatus (Columbus Instruments, Columbus, OH) rotating at 15 rpm. The amount of time that the mouse could stay on the rotarod before the first fall was recorded to determine disease onset. The duration of the rotarod test was 180 s, and was performed twice every week. A mouse was considered to fail the test when it could not stay on the rotarod for more than one standard error mean (>1 SEM) below the mean time period it stayed on the rotarod during the presymptomatic phase. The probability of passing the rotarod test was analyzed by Kaplan–Meier (n = 19 to 32 per genotype).

2.3.2. Grip strength

Hindlimb and forelimb strength were measured by a grip strength meter (Columbus Instruments, Columbus, OH) to determine disease progression. Mice were held by the base of the tail and were allowed to grasp a horizontal metal bar attached to the grip strength meter with their forelimbs or hindlimbs. They were gently pulled back horizontally. Mice resist the increasing force by clinging onto the metal bar until they can no longer resist the force. The force applied to the bar at the moment the mouse released the bar was recorded as its maximum force. The test was repeated three times and an average determined for each animal. The grip test was performed once each week from 80 days to 127 days of age (n = 5 to 10 per genotype).

2.3.3. Survival and disease duration

End stage of the disease was defined as the inability of the animal to right itself within 30 s after being placed on its side. Kaplan–Meier survival analysis was performed to compare survival between experimental groups (n = 22 to 32 per genotype). Disease duration was the mean time between age of disease onset, determined by rotarod test, and end stage of the disease (n = 19 to 32 per genotype).

2.4. Measurement of iron

The lumbar region of the spinal cord samples was harvested from 90-day (presymptomatic age) and 110-day-old (symptomatic age) SOD1 and SOD1/H67D mice. Presymptomatic and symptomatic ages were chosen based on behavior studies. Lumbar spinal cord samples from age-matched wild-type (WT) littermates were also harvested. The tissues were homogenized in RIPA buffer (Sigma, St. Louis, MO) with protease inhibitor cocktail (1:100; Sigma, St. Louis, MO). Total protein concentration was determined with Pierce BCA protein assay kit (Thermo scientific, MA). Iron concentrations (µg Fe/g of protein) were measured by graphite furnace atomic absorption spectrometry (model 5100AA, Perkin-Elmer, Norwalk, CT) according to standard protocol

[37]. Iron concentrations were measured in duplicates and averaged for each animal ($n = 7$ to 11 per genotype).

2.5. Histology

Ninety-, 110-day-old and end-stage mice were perfused transcardially with Ringer's solution followed by 4% paraformaldehyde in 0.1 M phosphate buffer. The spinal column was removed and post-fixed with 4% paraformaldehyde for 18 hours. The complete spinal cord was taken out and the lumbar region (L1–L5) was dissected.

2.5.1. Motor neuron loss

Paraffin embedded serial cross-sections ($6 \mu\text{m}$) were made from the lumbar region of the spinal cord samples. The sections were then processed for cresyl violet stain to determine motor neuron loss. Briefly, the sections were deparaffinized and rehydrated through a series of ethanol and the sections were stained with 0.5% cresyl violet (in distilled water) for 7 min. Excess stain was rinsed in distilled water and 70% ethanol. Sections were dehydrated by immersing in 95% ethanol followed by 100% ethanol. Glacial acetic acid (in 95% ethanol) was included during the dehydration series to differentiate the stain. Motor neurons in anterior gray matter of the lumbar region of the spinal cord were counted every 10th section with bright-field microscopy by an investigator blinded for genotype, using the following criteria: 1) the presence of a large single nucleolus located within the nucleus and 2) a cell soma area over $100 \mu\text{m}^2$. We also counted larger motor neurons with a cell soma area over $250 \mu\text{m}^2$ [38]. A total of ten sections were counted and averaged for each animal ($n = 7$ to 10 per genotype per age group).

2.5.2. Immunofluorescence staining

Paraffin embedded lumbar spinal cord sections ($n = 7$ to 10 per genotype per age group) were deparaffinized and rehydrated through a series of ethanol. Lumbar spinal cord sections were then processed with sodium citrate (pH 6.0) for antigen retrieval followed by 20-minute incubation with hydrogen peroxide (3.7% in methanol) at room temperature to block endogenous peroxidase activity. After blocking in 2% milk for one hour, sections were incubated with Iba-1 antibody alone (1:1000; Wako, Richmond, VA) or a mixture of SMI-32 (1:1000; Covance, Princeton, NJ) and TDP-43 (1:200; Proteintech, Chicago, IL) antibodies overnight at 4°C . Sections were then probed with fluorescently conjugated anti-host secondary antibodies (Alexa Fluor 488 (1:200) or a mixture of Alexa Fluor 488 (1:200) and Alexa Fluor 555 (1:200; Invitrogen, Grand Island, NY)) for one hour in the dark at room temperature. DAPI (1:1000) was used for nuclear staining. After washes, slides were mounted and were analyzed with fluorescence microscopy.

For L-ferritin and Iba-1 double immunofluorescence staining, because both L-ferritin and Iba-1 antibodies were made from the same host, L-ferritin was fluorescently labeled using a DyLight 550 antibody labeling kit (Thermo fisher scientific, Waltham, MA) prior to the incubation with spinal cord sections. Sections were first incubated with Iba-1 antibody overnight at 4°C , which was followed by an overnight incubation with DyLight labeled L-ferritin (1:200). Sections were then probed with Alexa Fluor 488 secondary antibody for one hour in the dark at room temperature. Spinal cord sections were analyzed with fluorescence microscopy.

2.6. Western Blot

The lumbar region of the spinal cord samples was harvested from presymptomatic age (90-day), symptomatic age (110-day) and end-stage SOD1/H67D mice ($n = 6$ to 10 per genotype). Samples from age-matched SOD1(G93A) and wild-type (WT) littermates were included in all of the analyses. Lumbar region of spinal cord tissues were homogenized in RIPA buffer (Sigma, St. Louis, MO) with protease inhibitor cocktail (1:100; Sigma, St. Louis, MO). Total protein

concentration was determined with Pierce BCA protein assay kit (Thermo scientific, MA). Total spinal cord homogenates ($20 \mu\text{g}$ total protein) was separated on 4–20% Criterion polyacrylamide Tris–HCl gel (Bio-Rad, Hercules, CA) by electrophoresis and transferred overnight at 4°C onto nitrocellulose membrane. For GFP protein analysis, total protein of $10 \mu\text{g}$ was loaded. After blocking with 5% nonfat dry milk, the membranes were incubated with a primary antibody for overnight at 4°C followed by an hour incubation with anti-host horseradish peroxidase-linked secondary antibodies (Amersham Bioscience, Piscataway, NJ). The signal was visualized with enhanced chemiluminescent (ECL) system (Perkin Elmer, Waltham, MA) and the densitometric analysis was performed with Multigauge software (V3.0; Fuji film system).

Lumbar region of spinal cord samples were analyzed for expressions of H-ferritin (1:1000; Covance, Princeton, NJ), L-ferritin (1:500; abcam, Cambridge, MA), transferrin receptor (TfR, 1:500; Zymed Laboratories Inc., San Francisco, CA), hemeoxygenase-1 (HO-1, 1:500; Enzo Life Science, Farmingdale, NY), nuclear factor E2-related factor 2 (Nrf2, 1:1000; abcam, Cambridge, MA), total caspase-3 (1:500; Cell Signaling Technology Inc., Danvers, MA), GFAP (1:10,000; Dako, Carpinteria, CA) and beta-actin (1:3000; Sigma, St. Louis, MO).

2.7. Statistical analyses

Data were expressed as mean \pm standard error. Kaplan–Meier was used to analyze the survival and probability of passing the rotarod test. An analysis of variance one-way ANOVA or two-way ANOVA (GraphPad Prism 4; La Jolla, CA) followed by Tukey multiple comparison or Bonferroni posttest was used to compare between experimental groups. For Grip strength analysis, repeated measure mixed ANOVA with Tukey–Kramer posttest was performed using SAS 9.3 (Cary, NC). A p -value < 0.05 was considered significance for all the experiments.

3. Results

3.1. H67D HFE shortens survival and accelerates disease progression

We determined survival, disease onset and disease progression in double transgenic (SOD1/H67D) mice and compared with SOD1 mice (G93A). The double transgenic mice had significantly shorter survival compared to SOD1 mice (Fig. 1 A). The median survival in double transgenic and SOD1 mutant mice was 128 days and 132.5 days respectively ($p = 0.02$). We found a gender effect on both survival and disease duration. The median survival of female double transgenic mice (129 days) was significantly shorter than female SOD1 mice (137 days; $p = 0.002$; Fig. 1 B). The median survival of males double transgenic (128 days) was not different from male SOD1 mice (122 days; $p = 0.17$; Fig. 1 C).

Disease duration, the time between disease onset and end-stage, was also shorter in double transgenic mice (21 ± 1.8 days; mean \pm SE) compared to SOD1 mice (26 ± 2.9 days); however, this difference did not reach statistical significance ($p = 0.11$; Fig. 2 A). When disease duration was analyzed by gender, females double transgenic (18 ± 1.4 days) exhibited significantly shorter disease duration than SOD1 mice (27 ± 3.6 days; mean \pm SE; $p = 0.02$; Fig. 2 B) though disease duration of males double transgenic (23 ± 3.3 days) was not different from male SOD1 mice (24 ± 4.9 days; $p = 0.78$; Fig. 2 C).

There was no difference between the SOD1 and double transgenic mice in age of disease onset as determined by performance on the rotarod ($p = 0.77$) (Fig. 3 A). The double transgenic and SOD1 mice failed the rotarod test starting at 107 ± 1.9 days and 106 ± 2.9 days respectively (mean \pm SE). The heterozygous H67D littermates (wt/H67D) were included in rotarod analysis as additional controls. Neither the wild-type (WT) nor the heterozygous H67D littermates (wt/H67D) failed the rotarod test during the observation period (not shown).

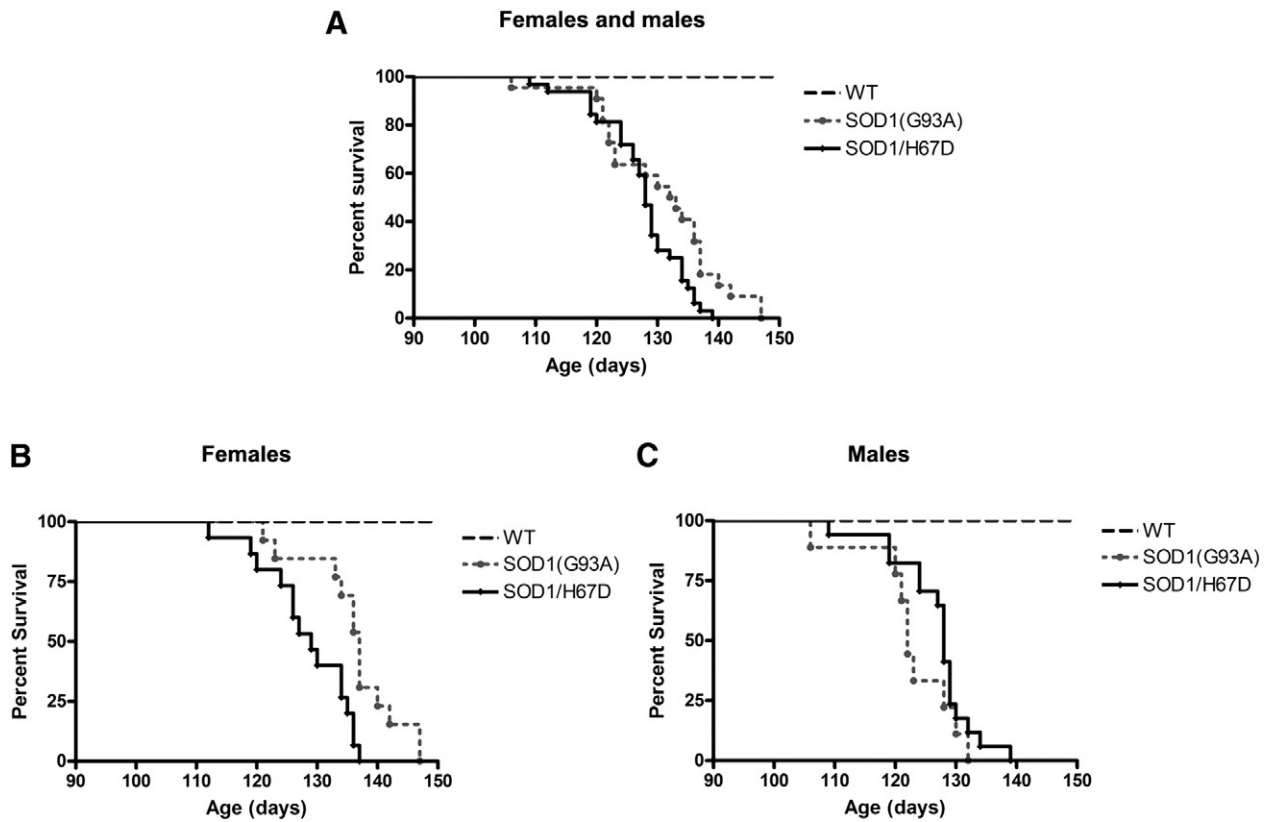


Fig. 1. H63D HFE shortens survival in double transgenic (SOD1/H67D) mice. Kaplan–Meier survival analysis comparing SOD1/H67D mice with SOD1(G93A) mice. Median survival of SOD1/H67D mice is shorter when compared with SOD1(G93A) mice (A, 128 days vs. 132.5 days, $n = 22$ to 32 per genotype, $p = 0.02$). Median survival of females SOD1/H67D mice is shorter compared to female SOD1(G93A) mice (B, 129 vs. 137 days, $n = 13$ to 15 per genotype, $p = 0.002$). Median survival of males SOD1/H67D and males SOD1(G93A) mice is not different (C, 128 vs. 122 days, $n = 9$ to 17 per genotype, $p = 0.17$).

Significant weakness in forelimbs and hindlimbs was observed in both double transgenic and SOD1 mice when compared with wild-type (WT) mice (Fig. 3 B–C). Compared to SOD1 mice, double transgenic mice performed significantly worse on both forelimb and hindlimb grip strength. Indeed, the double transgenic mice exhibited poorer forelimb and hindlimb strength than the SOD1 group beginning at the age of disease onset (106 days) until the end of the test (127 days) suggesting an accelerated disease progression in double transgenic mice. There was no gender effect on age of disease onset or progression as measured by rotarod and grip strength. The heterozygous H67D (wt/H67D) littermates exhibited no behavioral deficits nor muscle weakness or atrophy

in their limbs at any age. Therefore, wt/H67D mice are not included in further studies.

3.2. Motor neuron loss

Even before disease onset at 90 days of age, a significant loss of motor neurons was found in lumbar spinal cord of both the double transgenic and the SOD1 mice (27% loss in double transgenic mice compared to 21% loss in SOD1 mice), but the 6% greater loss of motor neurons in the double transgenic mice compared to SOD1 mice was not statistically significant (Fig. 4 A; $p = 0.55$). The motor neuron loss

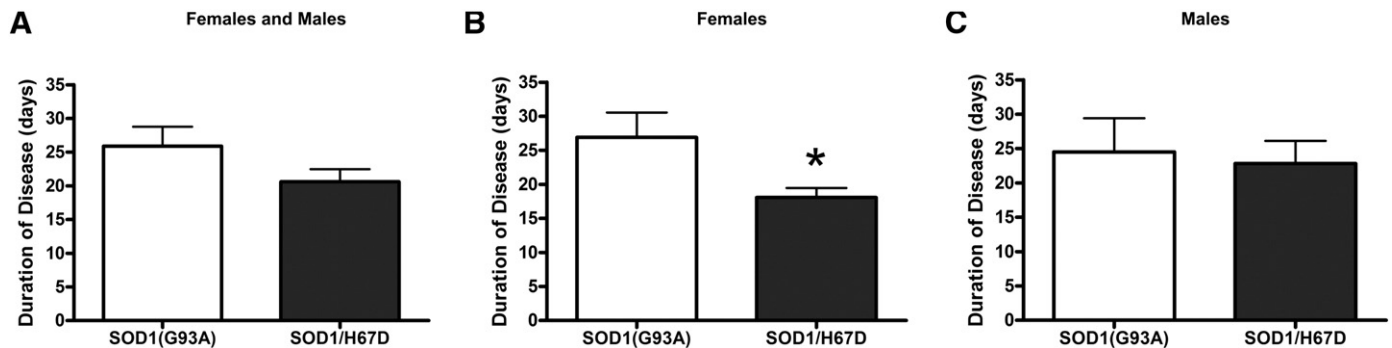


Fig. 2. Shorter disease duration in double transgenic (SOD1/H67D) mice. The SOD1/H67D mice tend to have shorter disease duration compared to SOD1(G93A) mice (A, 20.6 ± 1.9 days vs. 25.9 ± 2.8 days, $n = 19$ to 32, $p = 0.11$). There is a significantly shorter disease duration in females SOD1/H67D mice compared to females SOD1(G93A) mice (B, 18.1 ± 1.4 days vs. 26.9 ± 3.6 days, $n = 11$ to 15 per genotype, $*p < 0.05$). Disease duration in males SOD1/H67D is not different from male SOD1(G93A) mice (C, 22.8 ± 3.3 days vs. 24.5 ± 4.9 days, $n = 8$ to 17 per genotype, $p = 0.78$).

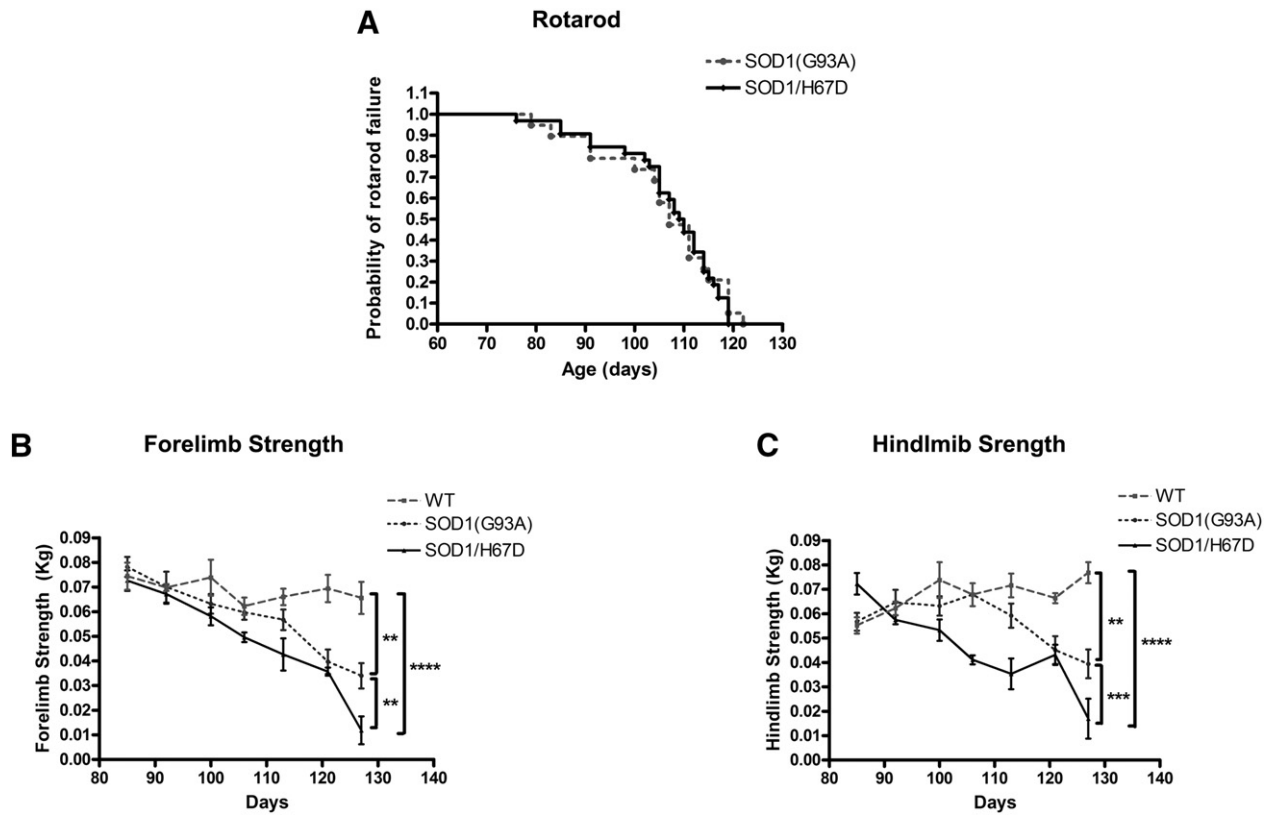


Fig. 3. Disease progression is accelerated in double transgenic (SOD1/H67D) mice. Kaplan–Meier analysis is used to compare the probability of passing the rotarod test (A) that defines the age of disease onset. Average age of disease onset is not different between SOD1/H67D and SOD1(G93A) mice (107 ± 1.9 days vs. 106 ± 2.8 days, $n = 19$ to 32 mice per genotype, $p = 0.77$). Grip strength meter was used to assess the strength of forelimbs (B) and hindlimbs (C). Disease groups have decreased forelimb and hindlimb strength over time compared to WT mice and there is a significant interaction between genotypes and time for both forelimb ($n = 5$ to 10 per genotype; $F(12, 115) = 3.35$; $p = 0.0003$) and hindlimb strength ($F(12, 115) = 5.95$; $p < 0.0001$). The SOD1/H67D mice have significantly less forelimb and hindlimb strength over time compared to SOD1(G93A) ($p = 0.003$ and $p = 0.0008$ respectively) and WT mice ($p < 0.0001$ and $p < 0.0001$ respectively). The SOD1(G93A) mice have lower forelimb and hindlimb strength than WT mice ($p = 0.0012$ and $p = 0.0021$ respectively) but stronger than SOD1/H67D mice. (** $p < 0.01$, *** $p < 0.001$, **** $p < 0.0001$).

continued to the 110 day time point, at which both double transgenic and SOD1 mice had lost about half of the motor neurons compared to WT mice (Fig. 4 B). There was no difference between double transgenic and SOD1 mice. Large motor neuron loss (a cell soma area over $250 \mu\text{m}^2$) was also present before disease onset at 90 days in both groups and was worsened with age. At 110 days, both double transgenic and SOD1 mice lost almost 3/4 of large motor neurons compared to WT mice. Large motor neuron loss was not different between the double transgenic and SOD1 mice at both 90 days ($p = 0.18$) and 110 days of

age ($p = 0.34$; data not shown). No gender difference was observed between groups.

3.3. Total iron concentrations are not altered in double transgenic (SOD1/H67D) mice

Total iron concentrations in lumbar spinal cords of 90 days and 110 days old SOD1 and double transgenic mice were measured to determine the impact of iron on disease progression in these mice. Iron

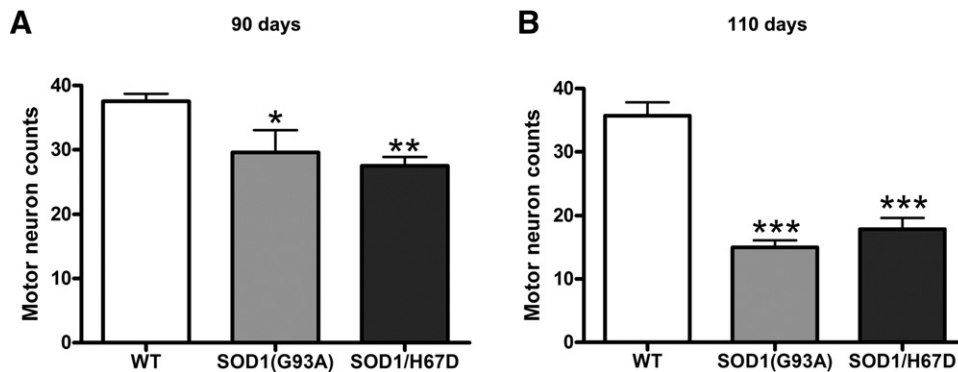


Fig. 4. Motor neuron loss in SOD1(G93A) and SOD1/H67D mice. Lumbar cord sections from 90- and 110-day-old mice were treated with cresyl violet stain. A significant loss of motor neurons ($>100 \mu\text{m}^2$) is observed in SOD1(G93A) and SOD1/H67D mice at both 90-days (A) and 110-days of age (B) but motor neuron loss in SOD1/H67D mice does not differ from SOD1(G93A) mice. Bars represent mean \pm standard error. (* $p < 0.05$, ** $p < 0.01$, *** $p < 0.001$ $n = 7$ to 10 per genotype).

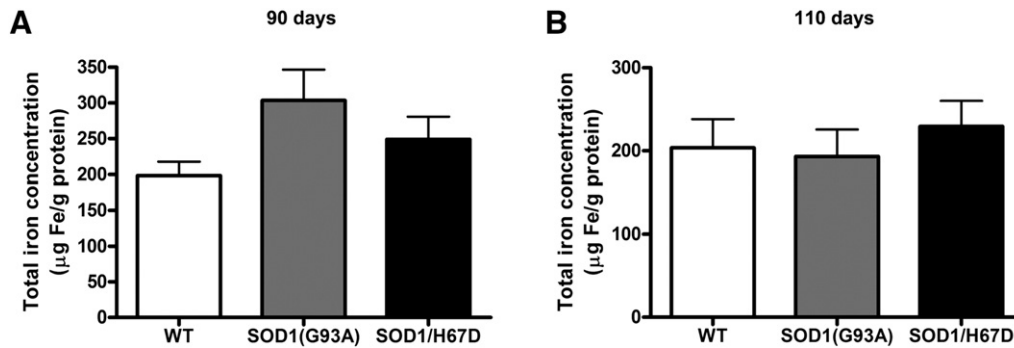


Fig. 5. Total iron concentrations are not different in spinal cords of double transgenic (SOD1/H67D) mice. Total iron concentrations in lumbar spinal cords of 90- and 110-day-old mice were measured with atomic absorption spectrometry. Iron levels in the lumbar spinal cords are not significantly different between groups at either time point. Bars represent mean \pm standard error. ($n = 7$ to 11 per genotype).

concentrations were also measured in lumbar spinal cords of age-matched WT mice. Total iron concentrations ($\mu\text{g Fe/g}$ of protein) are not different between groups at 90 days (presymptomatic age; Fig. 5 A) and 110 days when disease symptom exists (Fig. 5 B).

3.4. Altered iron management proteins expression in double transgenic (SOD1/H67D) mice

Compared to wild-type (WT) mice, a significant decrease in transferrin receptor (TfR) expression, a cellular iron uptake protein, was found in both double transgenic and SOD1 mice starting at 90 days (presymptomatic), and remained lower in both groups at 110 days (symptomatic) and end-stage (Fig. 6 A–C). Examination of the expression of L-ferritin, an iron storage protein particularly enriched in microglia, revealed a significant increase in the double transgenic mice compared to WT and the SOD1 mutant mice at both 90 and 110 days (Fig. 6 D–F). Compared to WT mice, L-ferritin expression was 49% higher in double transgenic mice at 90 days and remained increased with time to a maximal increase at end-stage (140% and 252% higher at 110 days and end-stage respectively). Notably, L-ferritin expression in double transgenic mice was 86% and 79% higher than SOD1 mice at 90 days and 110 days but was similar between the two groups at end stage. The similar levels of L-ferritin at end stage between the two groups resulted from a dramatic increase in L-ferritin in the SOD1 mice to those levels seen in the double transgenic. L-ferritin expression in SOD1 mice was significantly increased compared to WT only at end-stage (Fig. 6 D–F). H-ferritin expression in both double transgenic and SOD1 mice was not different from WT mice at any age (Fig. 6 G–I).

3.5. Increased microgliosis in double transgenic (SOD1/H67D) mice

To determine whether microgliosis is present in double transgenic mice, we performed immunofluorescence staining using an Iba-1 antibody. In wild-type mice at all observed ages, Iba-1 positive microglia in the lumbar spinal cords showed ramified or resting state morphology with long branching processes and a smaller cell body. However, microglia in both SOD1 and double transgenic mice showed activated morphology with shortening processes with a round enlarged cell body (Figs. 7 and 8). Interestingly, double transgenic mice have more number of activated microglia in the lumbar spinal cord compared to the SOD1 mice particularly at 110-days (Fig. 7 E–F), symptomatic age although the number of activated microglia in the ventral horn of lumbar spinal cords at 90-days (Fig. 7 B–C) and end-stage (Fig. 7 H–I) was similar between SOD1 and double transgenic mice. Because L-ferritin is primarily enriched in microglia [51], we performed double immunofluorescence staining to determine whether increased L-ferritin levels in double transgenic mice are also associated with increased microglial activation. Double immunofluorescence analyses indicate an increase L-ferritin staining in double transgenic mice, which is consistent with

findings from immunoblot analyses. Moreover L-ferritin is co-localized with Iba-1 positive microglia to greater extent in these mice (Fig. 8).

3.6. Increased caspase-3 in double transgenic (SOD1/H67D) mice

Caspase-3 expression in the lumbar spinal cords was not different between the three groups at 90 days (Fig. 9 A). However, at symptomatic age (110 days), caspase-3 expression was significantly increased in the double transgenic mice compared to WT and SOD1 mice (Fig. 9 B). At end-stage, caspase-3 expression was significantly increased in both double transgenic and SOD1 mice compared to WT mice. Caspase-3 expression was not different between double transgenic and SOD1 mice at end-stage (Fig. 9 C).

3.7. Increased gliosis in double transgenic (SOD1/H67D) mice

A significant increase in total GFAP expression was observed in lumbar spinal cords of both double transgenic and SOD1 mice starting at 90 days, presymptomatic age and remained higher at 110 days and at end-stage in both groups (Fig. 10 A–C). At symptomatic age (110 days), the magnitude of an increase in GFAP expression was higher in the double transgenic mice than SOD1 mice (126% increase vs. 78% increase compared to WT respectively; Fig. 10 B) but the differences between the double transgenic and the SOD1 mice did not reach statistical significance ($p = 0.13$).

3.8. Increased oxidative stress in double transgenic (SOD1/H67D) mice

We determined expressions of hemoxygenase-1 (HO-1) and nuclear factor E2-related factor 2 (Nrf2), as markers for oxidative stress in double transgenic mice. HO-1 expression was significantly increased in double transgenic mice compared to WT mice starting at 90 days and increased at each time point reaching maximal increase at end-stage (Fig. 11 A–C). The expression of HO-1 was greater in the double transgenic mice at 90 and 110 days compared with SOD1 mice (Fig. 11 A and B). The HO-1 expression in SOD1 mice was significantly increased compared to WT only at end-stage (Fig. 11 C) and was a result of a 5-fold increase in the levels of HO-1 in the end-stage of the SOD1 mice.

Next, we determined Nrf2 expression in these mice to test the impact of genotype on an antioxidant system. Expression of Nrf2 in double transgenic and SOD1 mice was not different from WT mice at 90 days; however, at the symptomatic (110 days) and end-stage time periods both double transgenic and SOD1 mice had significantly decreased Nrf2 expression compared to WT mice (Fig. 11 D–F). The Nrf2 expression in the lumbar spinal cords of double transgenic mice was 20% less than that in SOD1 mice at symptomatic age (110 days) although this difference did not reach statistical significance (Fig. 11 E).

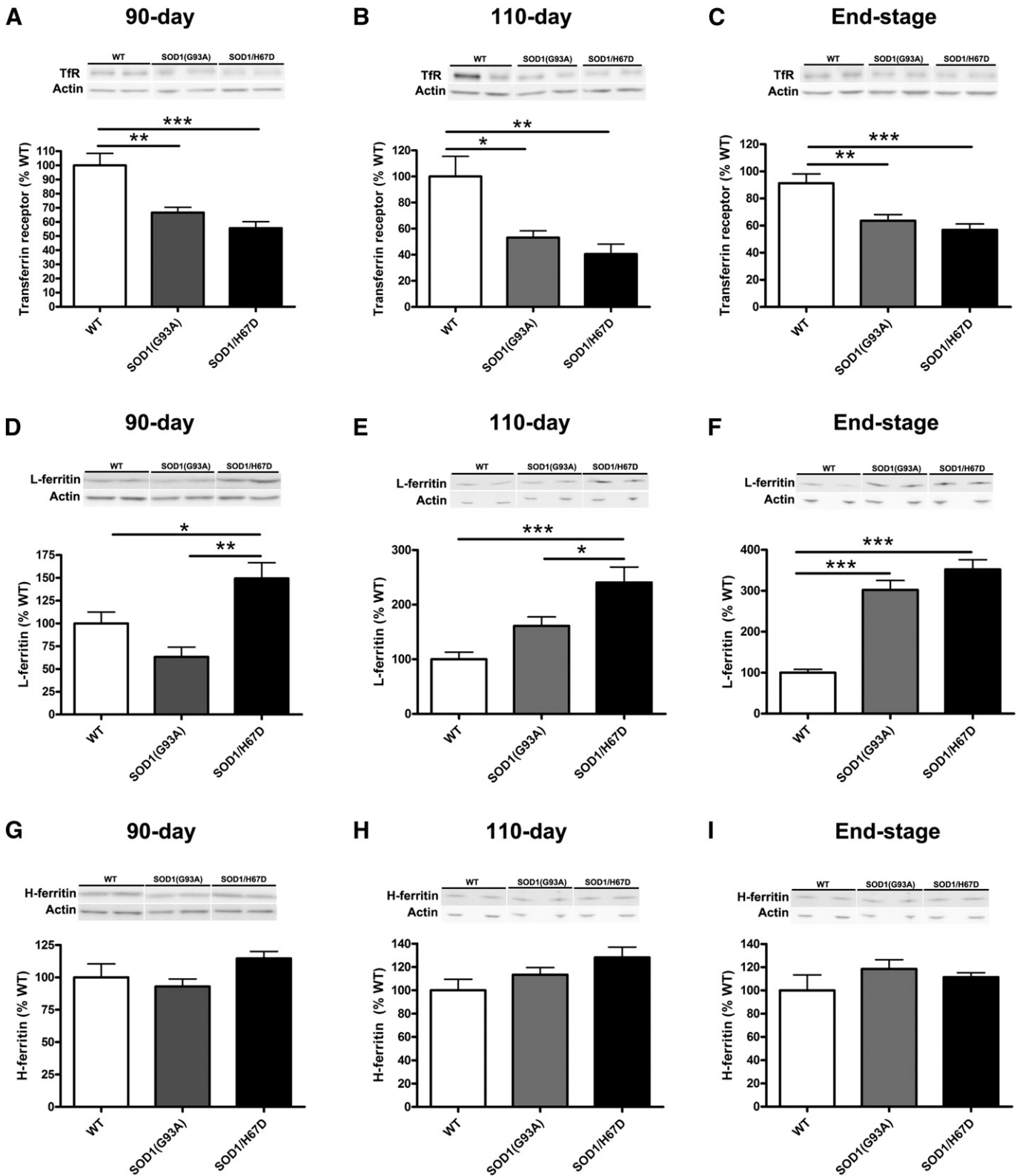


Fig. 6. Altered iron management protein expression in lumbar spinal cords of double transgenic (SOD1/H67D) mice. Lumbar spinal cord homogenates from 90-day, 110-day and end-stage SOD1/H67D, SOD1(G93A) and wild-type (WT) mice were determined for the expressions of transferrin receptor (TfR), L-ferritin and H-ferritin. A representative Western Blot gel is shown for each protein and the quantitative of blots is shown as a bar graph. The expression level is normalized to β -actin. Bars represent mean \pm standard error. (* $p < 0.05$, ** $p < 0.01$, *** $p < 0.001$; $n = 6$ to 10 per genotype). A–C. Transferrin receptor (TfR) expression in the lumbar spinal cords of SOD1/H67D and SOD1(G93A) mice is decreased at all ages compared to WT mice. D–F. L-ferritin expression is increased in the lumbar spinal cords of SOD1/H67D compared to SOD1(G93A) and wild-type mice at 90-days and 110-days. At end-stage, SOD1/H67D as well as SOD1(G93A) mice has significantly higher L-ferritin expression than WT mice. G–I. H-ferritin expression in SOD1/H67D and SOD1(G93A) mice do not differ from WT mice at all ages.

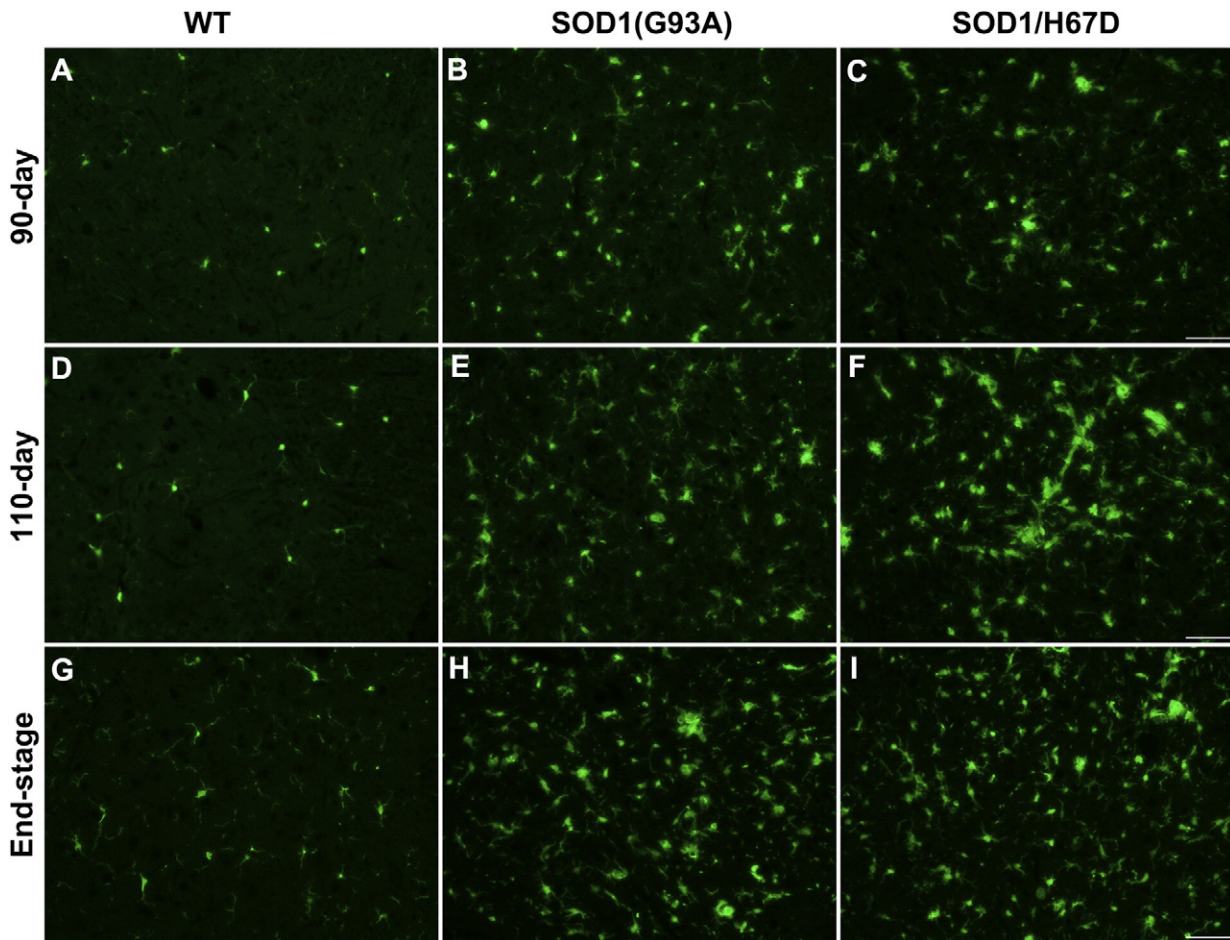


Fig. 7. Increased microgliosis in double transgenic (SOD1/H67D) mice. Lumbar spinal cord sections from 90-, 110-day and end-stage mice were stained for Iba-1 to detect microglia. Immunofluorescence analyses indicate that activated microglia were present in both SOD1(G93A) and SOD1/H67D mice compared to the wild-type mice at all observed ages. At 110-days, more activated microglia were observed in SOD1/H67D compared to SOD1(G93A) mice suggesting an increased microgliosis in SOD1/H67D mice at the symptomatic stage. The number of activated microglia in SOD1/H67D and SOD1(G93A) mice are similar at 90-days and end-stage ($n = 7$ to 10 per genotype per age group).

3.9. H67D HFE is not associated with altered nuclear localization of TDP-43 in double transgenic (SOD1/H67D) mice

TAR DNA binding protein 43 (TDP-43) has been reported to be the major pathological protein in ALS that mislocalizes to the cytoplasm where it is found as a major component of ubiquitin-positive neuronal cytoplasmic inclusions in ALS [5,39,40]. Therefore, we determined whether TDP-43 pathology is present in double transgenic mice by double immunofluorescence staining using TDP-43 and SMI-32 antibodies. TDP-43 was found in the nucleus of the healthy motor neurons in the lumbar spinal cords of WT mice at all ages investigated (Fig. 12 A, D, G). Consistent with previous studies [40–42], we found lack of TDP-43 mislocalization to the cytoplasm of motor neurons in SOD1 mice (Fig. 12 B, E, H). TDP-43 also did not mislocalize to the cytoplasm in double transgenic mice, and was found primarily in the nucleus of the remaining SMI-32-positive motor neurons in the lumbar spinal cords of these mice at all ages investigated (Fig. 12 C, F, I).

In the course of the analysis for TDP-43, we noted a consistent and dramatic difference in staining patterns following immunostaining with SMI-32 that we used for neuronal identification. Despite having similar SMI-32-positive motor neurons as SOD1, double transgenic mice have more disorganized neuronal processes in their lumbar spinal cords particularly at the end-stage of the disease compared to SOD1 mice (Fig. 12 H–I).

4. Discussion

In this study, we demonstrated that the combination of the H67D HFE gene variant with the SOD1 mutation shortens survival and accelerates disease progression compared to the SOD1 mutation alone. The presence of the H67D polymorphism altered iron homeostatic mechanism in the spinal cord of the mice as demonstrated by decreased TfR and increased L-ferritin expression. Moreover, the H-ferritin levels were similar in the double transgenic mice compared to WT mice despite significant neuronal cell loss. H-ferritin is predominantly expressed in neurons. Thus, the lack of a decrease in H-ferritin suggests the remaining neurons have increased H-ferritin suggesting this protein is offering protective function involving but perhaps not limited to neuronal iron accumulation. The alterations in iron homeostasis in the double transgenic model may contribute to increased oxidative stress, which in turn would support the gliosis and increased expression of caspase-3. Together we conclude that elevated oxidative stress, increased microglia activation and altered iron homeostasis are underlying mechanisms contributing to accelerated disease in double transgenic (SOD1/H67D) mice.

There is increasing evidence suggesting an association between H63D HFE and ALS [18–22]. Even studies in which a significant increase in H63D HFE was not found in ALS patients compared to the controls [23–25] the percentage of ALS patients with H63D HFE is consistently reported at around 30%. However, the impact of the HFE genotype on

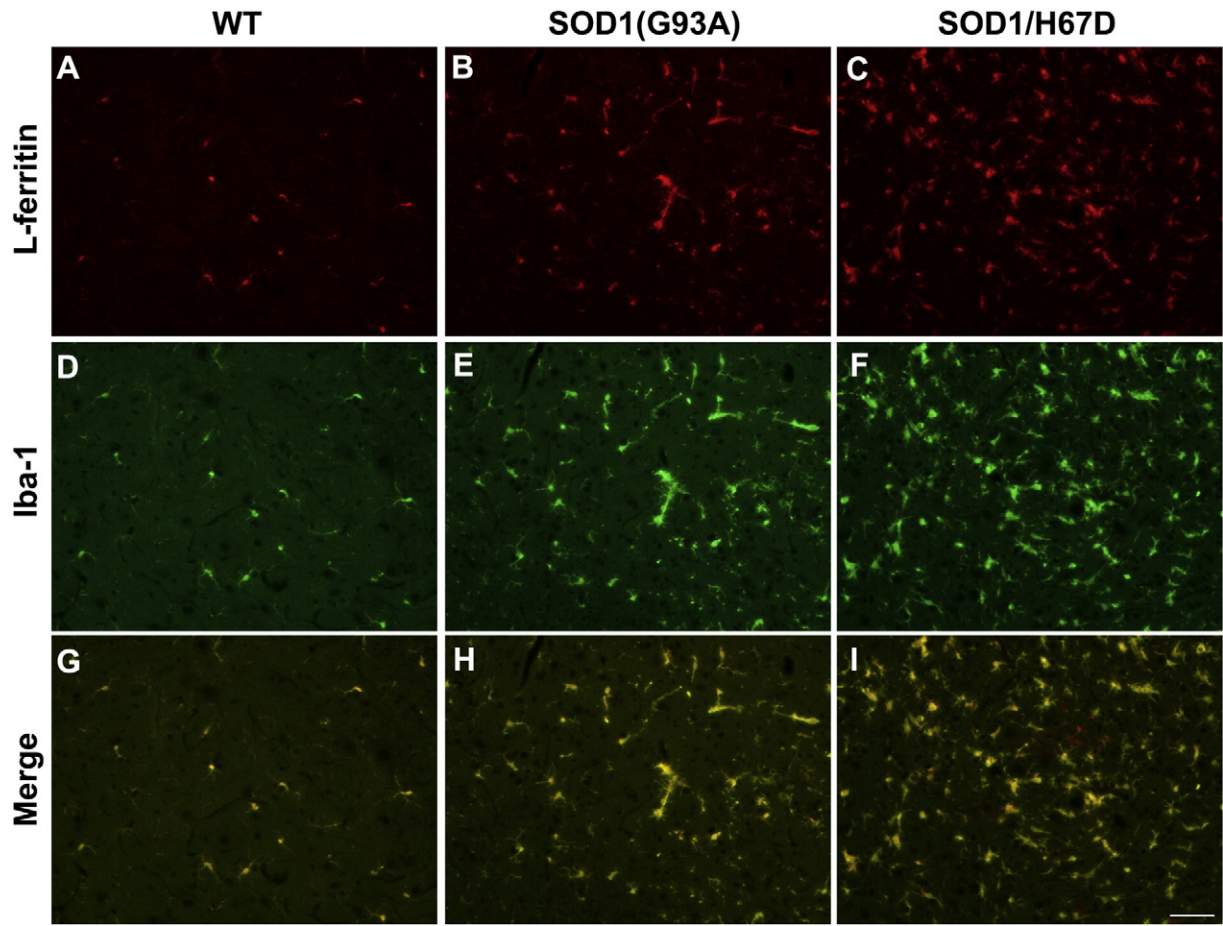


Fig. 8. Double immunofluorescence images for the colocalization of L-ferritin and Iba-1 positive microglia. Increased L-ferritin (A–C) and Iba-1 immunoreactivity (D–F) suggesting increased microgliosis in the lumbar spinal cords of double transgenic (SOD1/H67D) mice compared to WT and SOD1 mice at 110-days. Merged images (G–I) indicate the co-localization of L-ferritin with Iba-1 positive microglia to greater extent (n = 7 to 10 per genotype).

disease duration and survival is less established. Our findings of shorter survival and disease duration in an ALS mouse model with H67D HFE (SOD1/H67D) are not consistent with findings from ALS cases. In

human studies when heterozygous and homozygous for H63D HFE are pooled, presence of H63D HFE does not affect survival, age of disease onset, disease duration and site of onset in ALS patients [18–21,24,25].

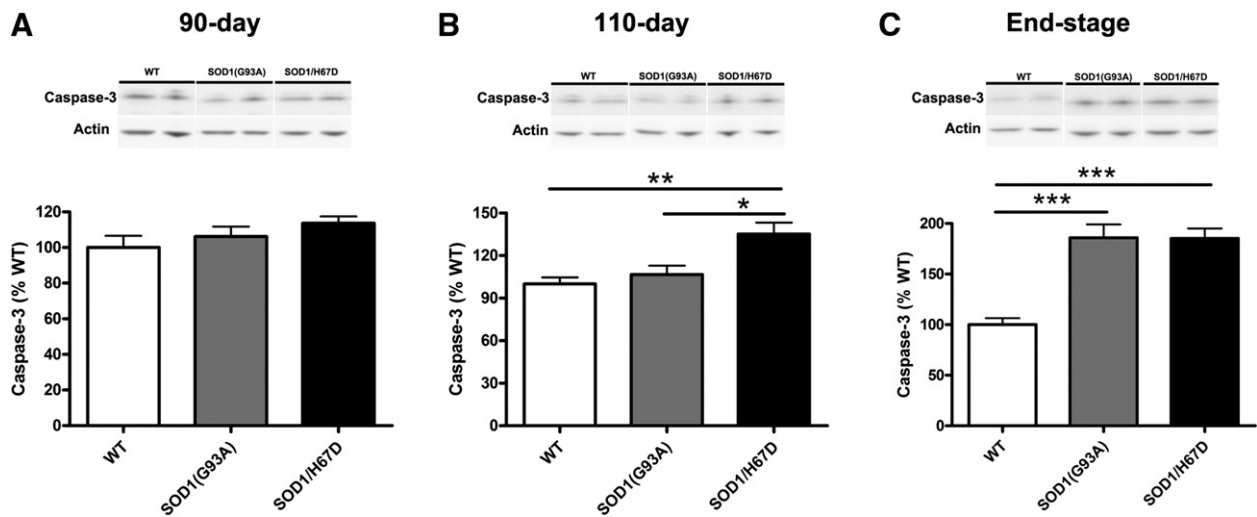


Fig. 9. Increased caspase-3 expression in lumbar spinal cords of SOD1/H67D. At 90-day, caspase-3 expression in lumbar spinal cords is not different between groups (A). At 110-days, SOD1/H67D mice have a significant increase in caspase-3 expression compared to WT and SOD1(G93A) mice (B). At end-stage, caspase-3 expression in both SOD1/H67D and SOD1(G93A) mice is increased compared to WT mice but caspase-3 expression in SOD1/H67D and SOD1(G93A) mice is not different (C). A representative Western Blot gel is shown for each protein and the quantitative of blots is shown as a bar graph. The expression level is normalized to β-actin. Bars represent mean ± standard error. (*p < 0.05, **p < 0.01, ***p < 0.001; n = 6 to 10 per genotype).

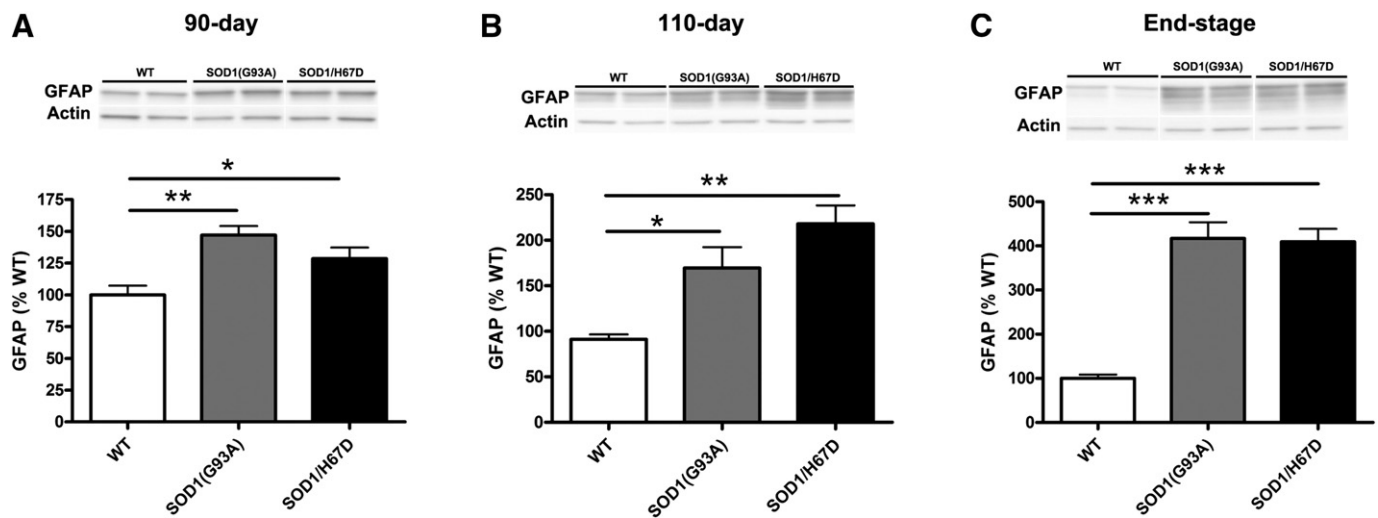


Fig. 10. Increased GFAP expression in lumbar spinal cords of SOD1/H67D. A significant increase in GFAP expression is observed in lumbar spinal cords of both SOD1/H67D and SOD1(G93A) mice starting at 90 days (A) and remains increased at 110 days (B) and end-stage (C). At 110 days, a magnitude of an increase in GFAP expression in double transgenic mice is higher compared with SOD1(G93A) mice. A representative Western Blot gel is shown for each protein and the quantitative of blots is shown as a bar graph. The expression level is normalized to β -actin. Bars represent mean \pm standard error. (* $p < 0.05$, ** $p < 0.01$, *** $p < 0.001$; $n = 6$ to 10 per genotype).

We have recently reported that ALS patients with homozygous for H63D HFE have increased disease duration [43]. However, the double transgenic mouse model combines mutations in a way not seen in the human studies that suggests when HFE is combined with a mutation in ALS the disease duration could be impacted. The difference between heterozygosity and homozygosity for the H63D variant may also be important. For example, in H67D knock-in mice homozygosity for H67D HFE induces adaptive mechanisms against increased oxidative stress although such adaptive responses are absent in heterozygous mice [31]. The lack of adaptive responses against cellular injury in heterozygotes may increase their vulnerability to cellular stress or toxicity induced by additional insults during disease conditions such as mutant SOD1-induced toxicity.

Genetic background can influence disease onset, severity, and survival in ALS rodent models independent of transgene copy numbers [44–46]. The double transgenic mice are on a C57BL6 background and this genetic background is associated with longer survival and milder disease phenotype [44–46], which is opposite from what we observed in double transgenic mice. Therefore, our results strongly suggest that H63D HFE is a contributing factor in ALS disease pathogenesis.

Mutations in the HFE protein are most commonly associated with elevated cellular iron uptake. Transferrin receptor (TfR) expression was decreased in the lumbar spinal cords of double transgenic mice from the presymptomatic stage through end-stage. Because TfR is expressed predominantly on neurons [47–49], the decrease could reflect the loss of neurons in the SOD1 and double transgenic mice. However, TfR is a cellular iron uptake protein and its expression is post-transcriptionally regulated by cellular iron status. Excess iron downregulates TfR protein synthesis while iron deficiency increases TfR synthesis [8,50]. Thus, decreased TfR expression in double transgenic mice could also be a response to altered iron homeostasis in the neurons of the double transgenic mice.

Similar to TfR, H-ferritin, an iron storage protein, is mainly expressed in neurons [51]. Although double transgenic mice have lost about half of their motor neurons compared to WT mice, total H-ferritin levels are not significantly different. This suggests H-ferritin expression may be increased in surviving neurons, reflecting a protective response for neurons during stress in the double transgenic mice. Moreover, L-ferritin expression is dramatically increased in the double transgenic mice even before disease onset. L-ferritin is a long-term iron storage

protein primarily enriched in microglia [51]. Ferritin synthesis is post-transcriptionally regulated by iron status [50]. Therefore, higher L-ferritin levels in double transgenic mice than in SOD1 mice further suggests altered iron homeostasis in the spinal cord of these mice.

In addition to iron dyshomeostasis, pro-inflammatory cytokines associated with activated microglia can increase L-ferritin expression in these cells [52]. Because neuroinflammation is a pathological hallmark in ALS and increased inflammatory cytokines together with microgliosis are present in ALS [53,54], the increase in L-ferritin suggests that additional influences, such as microglial toxicity or inflammation, may contribute to accelerated disease in double transgenic mice. Indeed, immunofluorescence analyses demonstrating increase Iba-1 immunoreactivity as well as a strong co-localization of L-ferritin with Iba-1 positive microglia further indicate that increased microgliosis contributes to accelerated disease in double transgenic mice.

Additional evidence suggesting the role of microgliosis in accelerated disease in double transgenic mice is an increase in caspase-3 expression without additional motor neuron loss compared to SOD1 mice. Although caspase-3 activation is well accepted as a downstream event in the apoptotic pathway, a non-apoptotic role of caspase-3 in regulating microglial activation and neurotoxicity has been reported. Activating microglia with immunogens such as lipopolysaccharide increases expressions of caspase-3, -7 and -8 without microglial cell death. By inhibiting caspases, microglial activation is blocked and its associated neuronal toxicity is reduced [55]. Although we cannot exclude the possibility of increased caspase-3 and apoptosis in microglia, our data suggest that increased caspase-3 in double transgenic mice is associated with increased microglial activation, which is consistent with increased L-ferritin levels and Iba-1 immunoreactivity in these mice. Given that damage in microglia mainly affects disease progression, whereas motor neurons toxicity affects disease onset [56,57], the observations of accelerated disease progression together with increased L-ferritin, Iba-1 immunoreactivity and caspase-3 expression strongly implicates microglial activation as a mechanism underlying accelerated disease progression in the double transgenic mice.

An additional change in glia in double transgenic mice is astrogliosis indicated by increased GFAP expression. Astrogliosis is a known pathological hallmark of ALS. Similar to microglia, damage in astrocytes mainly affects disease progression without influencing disease onset in ALS [57]. In ALS animal models astrogliosis appears before disease onset [57]. Consistently, in our study, increased GFAP expression was present

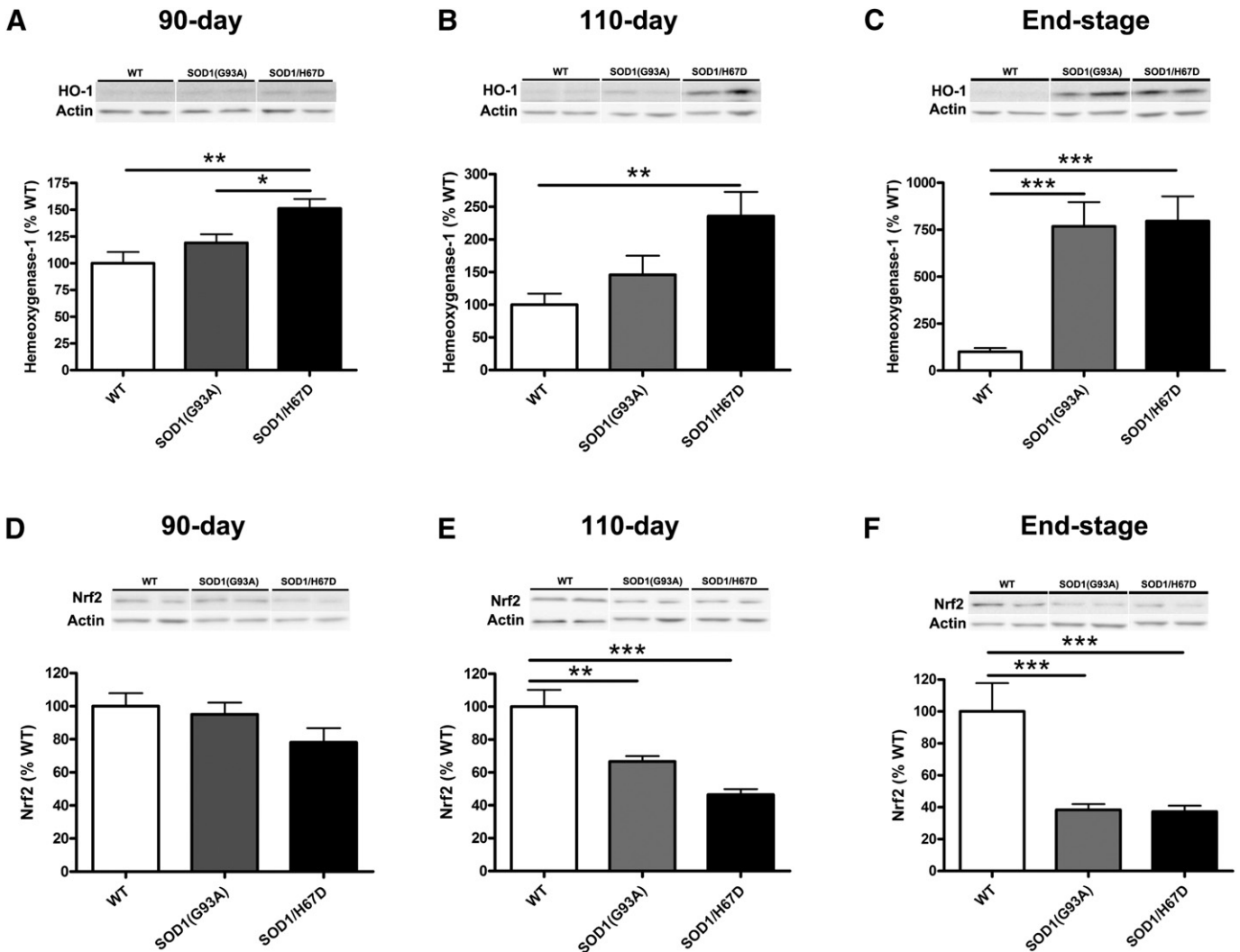


Fig. 11. Increased oxidative stress in lumbar spinal cords of double transgenic (SOD1/H67D) mice. Lumbar spinal cord homogenates from 90-day, 110-day and end-stage SOD1/H67D, SOD1(G93A) and wild-type (WT) mice were determined for the expressions of hemoxygenase-1 (HO-1) and nuclear factor E2-related factor 2 (Nrf2), as markers of oxidative stress. A representative Western Blot gel is shown for each protein and the quantitative of blots is shown as a bar graph. The expression level is normalized to β -actin. Bars represent mean \pm standard error. (* $p < 0.05$, ** $p < 0.01$, *** $p < 0.001$; $n = 6$ to 10 per genotype). A–C. Increased hemoxygenase-1 (HO-1) expression is found in lumbar spinal cords of SOD1/H67D compared to WT mice at 90 days (A), 110 days (B) and end-stage (C). HO-1 expression in SOD1(G93A) mice is increased only at end-stage when compared to WT mice. D–F. The Nrf2 expression is not different between groups at 90 days (D). Nrf2 expression is decreased in SOD1/H67D and SOD1(G93A) mice at 110 days (E) and at end-stage (F). At 110 days, Nrf2 expression is decreased by 20% in SOD1/H67D compared to SOD1(G93A) mice; whereas, Nrf2 expression in both group is not different at end-stage.

in double transgenic and SOD1 mice before disease onset, and then progressively increased; however, the magnitude of the increase in GFAP was higher in double transgenic mice, particularly at the symptomatic stage. Activated astrocytes can mediate motor neuron toxicity by secreting soluble factors toxic to motor neurons [58] and by enhancing microglial inflammatory responses [57]. Therefore, elevated astrogliosis in the double transgenic mice may contribute to increased neuronal toxicity and microglial inflammatory responses, further contributing to an accelerated disease.

Moreover, alterations in iron homeostasis and inflammatory environments are associated with oxidative stress, a significant part of the disease processes in ALS. We previously demonstrated that H63D HFE creates an environment for oxidative stress [31,59]. In this study, oxidative stress, indicated by increased HO-1 and decreased Nrf2, is present in both double transgenic and SOD1 mice. However, the magnitude of the changes, particularly at the symptomatic stage, is greater in double transgenic mice than in SOD1 mice. The decrease in Nrf2, which regulates cellular antioxidant responses [60] in double transgenic mice compared to SOD1 mice, is particularly noteworthy as potentially part of ALS pathogenesis. Previous studies have reported decreased Nrf2

expression in postmortem brain and spinal cord tissues from sporadic ALS patients [61] and in SOD1(G93A) motor neurons [62]. Decreased Nrf2 also increases motor neuron sensitivity to nerve growth factor induced apoptosis [62]. Upregulating antioxidant genes by Nrf2 activators slow disease progression in an ALS mouse model [63]. These reports together with our findings suggest that the decreased Nrf2 levels in double transgenic mice compared to SOD1 mice may be a driver of the accelerated disease in the double transgenic mice, possibly by reducing levels of glutathione (GSH), an important anti-oxidant protein downstream from Nrf2 [60,64]. Indeed, decreased GSH in the ALS mouse model accelerates disease and shortens survival due to increased oxidative stress [65], findings similar to those we observed in double transgenic mice in this study.

An additional pathogenic change in ALS is mislocalization of TDP-43, which is normally a nuclear protein, to the cytoplasm where it is found as a component of ubiquitin-positive neuronal inclusions [5,39,40,42]. Also, recent studies have reported TDP-43 as one of the major pathological proteins in ALS [5,39]. Because mislocalization of TDP-43 to the cytoplasm correlates with rapid clinical course in ALS [66] and double transgenic mice in this study have a more rapid disease profile, we

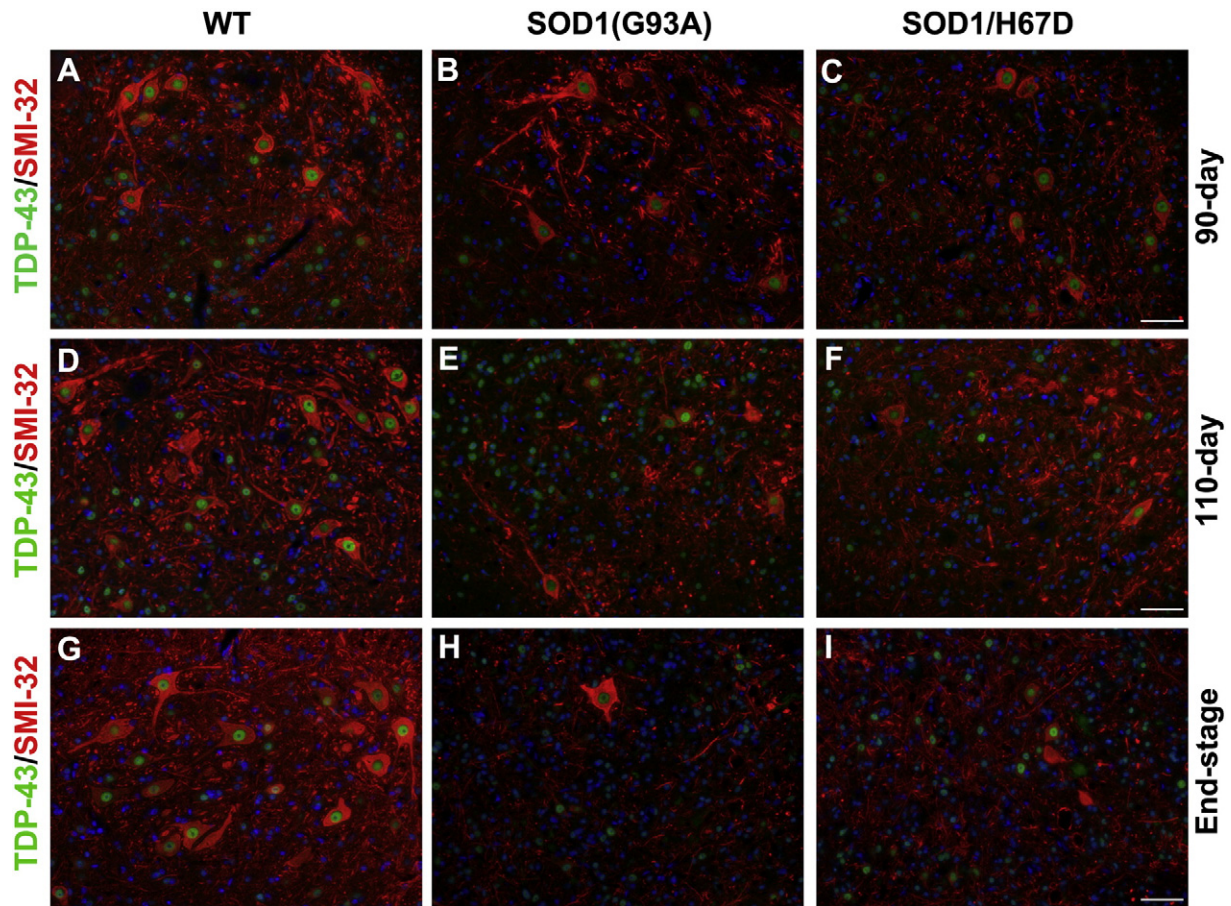


Fig. 12. H67D HFE does not disrupt nuclear localization of TDP-43 in double transgenic (SOD1/H67D) mice. Representative immunofluorescence images of lumbar spinal cords from 90-, 110-day and end-stage mice stained with TDP-43 (green), SMI-32 (red) and DAPI (blue). There are less SMI-32 positive motor neurons (red) in the lumbar spinal cords of SOD1(G93A) and SOD1/H67D mice compared to the wild-type mice at all observed ages. Similar to findings in the wild-type mice (A, D, G), TDP-43 remains localized primarily to the nucleus of surviving motor neurons in both SOD1(G93A) (B, E, H) and SOD1/H67D mice (C, F, I) at all ages ($n = 4$ to 6 per genotype per age group). It is noted in the course of the evaluation for TDP-43 that there was a dramatic difference in the appearance of the SMI-32 immunostaining pattern in the double transgenic mice compared to the wild-type or SOD1 mutant mice. The staining pattern in the wild-type is very regular whereas there is limited staining of filaments in the SOD1 mice, consistent with the significant cell death observed. In the double transgenic mice, there is more neurofilament staining in processes (despite similar amount of cell death to the SOD1 mice) particularly at the 110 day and end-stage time periods (E–I).

performed double immunofluorescence staining to clarify whether mislocalization of TDP-43 is present in double transgenic mice. TDP-43 was found primarily in the nucleus of the remaining motor neurons even at disease end-stage in double transgenic mice. The lack of TDP-43 mislocalization in the double transgenic mice is similar to that reported in the SOD1 mutation alone [40–42] and consistent with our observations in this study. The lack of mislocalization of TDP-43 to the cytoplasm implicates that the pathological TDP-43 is unlikely to contribute as a mechanism underlying accelerated disease in double transgenic mice but also demonstrates that accelerated disease can occur in the absence of TDP-43 cytological changes.

Although TDP-43 immunostaining pattern is similar between double transgenic and SOD1 mice, we found a different SMI-32 immunostaining pattern between the two groups, particularly at end-stage of the disease. SMI-32 is a marker for non-phosphorylated heavy-chain neurofilament protein (NFH). Abnormal accumulation of neurofilament proteins in the cell body and proximal axons of motor neurons, and defective axonal transport are consistent pathological hallmarks of ALS [67,68]. A mutation in NFH gene is found in sporadic ALS cases [69]. Higher levels of phosphorylated NFH are found in cerebrospinal fluid (CSF) [70–72] and plasma samples of ALS patients [73]. Moreover, CSF and plasma phosphorylated NFH levels are correlated with disease progression in ALS patients [70,72,73]. Another neurofilament subunit,

light-chain neurofilament, levels are also elevated in the CSF of ALS patients [71,74,75]. Although detailed analyses of neurofilament pathology in double transgenic mice is beyond the scope of this study, more SMI-32-positive disorganized neuronal processes observed in the spinal cords of these mice may suggest altered phosphorylation of neurofilament proteins and impaired axonal transport in double transgenic mice.

In summary, we determined the impact of H67D HFE on ALS pathogenesis by generating a double transgenic mouse line (SOD1/H67D). There are two important findings in this study. First, H67D shortens survival and accelerates disease progression in double transgenic mice. Importantly, double transgenic mice have accelerated disease progression in the absence of environmental stressors or challenges that may impact ALS onset such as inflammation, diet or toxic exposure. Secondly, the addition of the H67D HFE gene variant to the SOD1 mouse model of ALS alters iron metabolism, increases oxidative stress and microglial toxicity, and is associated with neurofilament disruption, which are underlying mechanisms associated with shorter survival and accelerated disease progression. The disruption of cellular functions in double transgenic mice is more extensive than that in mice with SOD1(G93A) alone. Because H67D HFE is present in as many as 30% of ALS patients, the double transgenic mouse model could serve as a preclinical model to assess the impact of a common genetic variant on disease progression and treatment strategies.

Conflict of interest

The authors declare no competing financial interests.

Acknowledgements

This work is supported by Judith and Jean Pape Adams Charitable Foundation. The authors also acknowledge the Paul and Harriett Campbell Fund for ALS research, Zimmerman Family Love Fund and the Robert Luongo ALS Fund for their generous support.

References

- [1] L. Ferraiuolo, J. Kirby, A.J. Grierson, M. Sendtner, P.J. Shaw, Molecular pathways of motor neuron injury in amyotrophic lateral sclerosis, *Nat. Rev. Neurol.* 7 (2011) 616–630.
- [2] W. Robberecht, T. Philips, The changing scene of amyotrophic lateral sclerosis, *Nat. Rev. Neurosci.* 14 (2013) 248–264.
- [3] L. Regal, L. Vanopdenbosch, P. Tilkin, L. Van den Bosch, V. Thijs, R. Sciot, W. Robberecht, The G93C mutation in superoxide dismutase 1: clinicopathologic phenotype and prognosis, *Arch. Neurol.* 63 (2006) 262–267.
- [4] D.R. Rosen, T. Siddique, D. Patterson, D.A. Figlewicz, P. Sapp, A. Hentati, D. Donaldson, J. Goto, J.P. O'Regan, H.X. Deng, et al., Mutations in Cu/Zn superoxide dismutase gene are associated with familial amyotrophic lateral sclerosis, *Nature* 362 (1993) 59–62.
- [5] M. Neumann, D.M. Sampathu, L.K. Kwong, A.C. Truax, M.C. Micsenyi, T.T. Chou, J. Bruce, T. Schuck, M. Grossman, C.M. Clark, L.F. McCluskey, B.L. Miller, E. Masliah, I.R. Mackenzie, H. Feldman, W. Feiden, H.A. Kretschmar, J.Q. Trojanowski, V.M. Lee, Ubiquitinated TDP-43 in frontotemporal lobar degeneration and amyotrophic lateral sclerosis, *Science* 314 (2006) 130–133.
- [6] T.J. Kwiatkowski Jr., D.A. Bosco, A.L. Leclerc, E. Tamrazian, C.R. Vanderburg, C. Russ, A. Davis, J. Gilchrist, E.J. Kasarskis, T. Munsat, P. Valdmanis, G.A. Rouleau, B.A. Hosler, P. Cortelli, P.J. de Jong, Y. Yoshinaga, J.L. Haines, M.A. Pericak-Vance, J. Yan, N. Ticozzi, T. Siddique, D. McKenna-Yasek, P.C. Sapp, H.R. Horvitz, J.E. Landers, R.H. Brown Jr., Mutations in the FUS/TLS gene on chromosome 16 cause familial amyotrophic lateral sclerosis, *Science* 323 (2009) 1205–1208.
- [7] M. DeJesus-Hernandez, I.R. Mackenzie, B.F. Boeve, A.L. Boxer, M. Baker, N.J. Rutherford, A.M. Nicholson, N.A. Finch, H. Flynn, J. Adamson, N. Kouri, A. Wojtas, P. Sengdy, G.Y. Hsiung, A. Karydas, W.W. Seeley, K.A. Josephs, G. Coppola, D.H. Geschwind, Z.K. Wszolek, H. Feldman, D.S. Knopman, R.C. Petersen, B.L. Miller, H.W. Dickson, K.B. Boylan, N.R. Graff-Radford, R. Rademakers, Expanded GGGGCC hexanucleotide repeat in noncoding region of C9ORF72 causes chromosome 9p-linked FTD and ALS, *Neuron* 72 (2011) 245–256.
- [8] S. Oshiro, M.S. Morioka, M. Kikuchi, Dysregulation of iron metabolism in Alzheimer's disease, Parkinson's disease, and amyotrophic lateral sclerosis, *Adv. Pharmacol. Sci.* 2011 (2011) 378278.
- [9] H. Oba, T. Araki, K. Ohtomo, S. Monzawa, G. Uchiyama, K. Koizumi, Y. Nogata, K. Kachi, Z. Shiozawa, M. Kobayashi, Amyotrophic lateral sclerosis: T2 shortening in motor cortex at MR imaging, *Radiology* 189 (1993) 843–846.
- [10] E.J. Kasarskis, L. Tandon, M.A. Lovell, W.D. Ehmann, Aluminum, calcium, and iron in the spinal cord of patients with sporadic amyotrophic lateral sclerosis using laser microprobe mass spectroscopy: a preliminary study, *J. Neurol. Sci.* 130 (1995) 203–208.
- [11] E.F. Goodall, M.S. Haque, K.E. Morrison, Increased serum ferritin levels in amyotrophic lateral sclerosis (ALS) patients, *J. Neurol.* 255 (2008) 1652–1656.
- [12] M. Qureshi, R.H. Brown Jr., J.T. Rogers, M.E. Cudkowicz, Serum ferritin and metal levels as risk factors for amyotrophic lateral sclerosis, *Open Neurol. J.* 2 (2008) 51–54.
- [13] Y. Nadjar, P. Gordon, P. Corcia, G. Bensimon, L. Pieroni, V. Meininger, F. Salachas, Elevated serum ferritin is associated with reduced survival in amyotrophic lateral sclerosis, *PLoS One* 7 (2012) e45034.
- [14] S.Y. Jeong, K.I. Rathore, K. Schulz, P. Ponka, P. Arosio, S. David, Dysregulation of iron homeostasis in the CNS contributes to disease progression in a mouse model of amyotrophic lateral sclerosis, *J. Neurosci.* 29 (2009) 610–619.
- [15] Q. Wang, X. Zhang, S. Chen, S. Zhang, M. Youdim, W. Le, Prevention of motor neuron degeneration by novel iron chelators in SOD1(G93A) transgenic mice of amyotrophic lateral sclerosis, *Neurodegener. Dis.* 8 (2011) 310–321.
- [16] A.T. Merryweather-Clarke, J.J. Pointon, J.D. Shearman, K.J. Robson, Global prevalence of putative haemochromatosis mutations, *J. Med. Genet.* 34 (1997) 275–278.
- [17] W. Nandar, J.R. Connor, HFE gene variants affect iron in the brain, *J. Nutr.* 141 (2011) 729S–739S.
- [18] X.S. Wang, S. Lee, Z. Simmons, P. Boyer, K. Scott, W. Liu, J. Connor, Increased incidence of the Hfe mutation in amyotrophic lateral sclerosis and related cellular consequences, *J. Neurol. Sci.* 227 (2004) 27–33.
- [19] E.F. Goodall, M.J. Greenway, I. van Marion, C.B. Carroll, O. Hardiman, K.E. Morrison, Association of the H63D polymorphism in the hemochromatosis gene with sporadic ALS, *Neurology* 65 (2005) 934–937.
- [20] G. Restagno, F. Lombardo, P. Ghiglione, A. Calvo, E. Cocco, L. Sbaiz, R. Mutani, A. Chio, HFE H63D polymorphism is increased in patients with amyotrophic lateral sclerosis of Italian origin, *J. Neurol. Neurosurg. Psychiatry* 78 (2007) 327.
- [21] N.A. Sutedja, R.J. Sinke, P.W. Van Vught, M.W. Van der Linden, J.H. Wokke, C.M. Van Duijn, O.T. Njajou, Y.T. Van der Schouw, J.H. Veldink, L.H. Van den Berg, The association between H63D mutations in HFE and amyotrophic lateral sclerosis in a Dutch population, *Arch. Neurol.* 64 (2007) 63–67.
- [22] X. He, X. Lu, J. Hu, J. Xi, D. Zhou, H. Shang, L. Liu, H. Zhou, B. Yan, L. Yu, F. Hu, Z. Liu, L. He, X. Yao, Y. Xu, H63D polymorphism in the hemochromatosis gene is associated with sporadic amyotrophic lateral sclerosis in China, *Eur. J. Neurol.* 18 (2011) 359–361.
- [23] A.A. Yen, E.P. Simpson, J.S. Henkel, D.R. Beers, S.H. Appel, HFE mutations are not strongly associated with sporadic ALS, *Neurology* 62 (2004) 1611–1612.
- [24] J. Praline, H. Blasco, P. Vourch, V. Rat, C. Gendrot, W. Camu, C.R. Andres, Study of the HFE gene common polymorphisms in French patients with sporadic amyotrophic lateral sclerosis, *J. Neurol. Sci.* 317 (2012) 58–61.
- [25] W. van Rheezen, F.P. Diekstra, P.T. van Doormaal, M. Seelen, K. Kenna, R. McLaughlin, A. Shatunov, D. Czell, M.A. van Es, P.W. van Vught, P. van Damme, B.N. Smith, S. Waibel, H.J. Schelhaas, A.J. van der Kooi, M. de Visser, M. Weber, W. Robberecht, O. Hardiman, P.J. Shaw, C.E. Shaw, K.E. Morrison, A. Al-Chalabi, P.M. Andersen, A.C. Ludolph, J.H. Veldink, L.H. van den Berg, H63D polymorphism in HFE is not associated with amyotrophic lateral sclerosis, *Neurobiol. Aging* 34 (2013) 1517 (e1515–1517).
- [26] C. Ellervik, H. Birgens, A. Tybjaerg-Hansen, B.G. Nordestgaard, Hemochromatosis genotypes and risk of 31 disease endpoints: meta-analyses including 66,000 cases and 226,000 controls, *Hepatology* 46 (2007) 1071–1080.
- [27] J.E. Nielsen, L.N. Jensen, K. Krabbe, Hereditary haemochromatosis: a case of iron accumulation in the basal ganglia associated with a parkinsonian syndrome, *J. Neurol. Neurosurg. Psychiatry* 59 (1995) 318–321.
- [28] D. Berg, U. Hoggemuller, E. Hofmann, R. Fischer, M. Kraus, M. Scheurlen, G. Becker, The basal ganglia in haemochromatosis, *Neuroradiology* 42 (2000) 9–13.
- [29] G. Bartzokis, P.H. Lu, T.A. Tishler, D.G. Peters, A. Kosenko, K.A. Barrall, J.P. Finn, P. Villablanca, G. Laub, L.L. Altschuler, D.H. Geschwind, J. Mintz, E. Neely, J.R. Connor, Prevalent iron metabolism gene variants associated with increased brain ferritin iron in healthy older men, *J. Alzheimers Dis.* 20 (2010) 333–341.
- [30] G. Bartzokis, P.H. Lu, K. Tingus, D.G. Peters, C.P. Amar, T.A. Tishler, J.P. Finn, P. Villablanca, L.L. Altschuler, J. Mintz, E. Neely, J.R. Connor, Gender and iron genes may modify associations between brain iron and memory in healthy aging, *Neuropsychopharmacology* 36 (2011) 1375–1384.
- [31] W. Nandar, E.B. Neely, E. Unger, J.R. Connor, A mutation in the HFE gene is associated with altered brain iron profiles and increased oxidative stress in mice, *Biochim. Biophys. Acta* 1832 (2013) 729–741.
- [32] F. Ali-Rahmani, P.S. Grigson, S. Lee, E. Neely, J.R. Connor, C.L. Schengrund, H63D mutation in hemochromatosis alters cholesterol metabolism and induces memory impairment, *Neurobiol. Aging* 35 (2014) 1511 (e1511–1512).
- [33] S.Y. Lee, S.M. Patton, R.J. Henderson, J.R. Connor, Consequences of expressing mutants of the hemochromatosis gene (HFE) into a human neuronal cell line lacking endogenous HFE, *FASEB J.* 21 (2007) 564–576.
- [34] R.M. Mitchell, S.Y. Lee, Z. Simmons, J.R. Connor, HFE polymorphisms affect cellular glutamate regulation, *Neurobiol. Aging* 32 (2011) 1114–1123.
- [35] Y. Liu, S.Y. Lee, E. Neely, W. Nandar, M. Moyo, Z. Simmons, J.R. Connor, Mutant HFE H63D protein is associated with prolonged endoplasmic reticulum stress and increased neuronal vulnerability, *J. Biol. Chem.* 286 (2011) 13161–13170.
- [36] J.D. Rothstein, Current hypotheses for the underlying biology of amyotrophic lateral sclerosis, *Ann. Neurol.* 65 (Suppl. 1) (2009) S3–S9.
- [37] K.M. Erikson, D.J. Pinero, J.R. Connor, J.L. Beard, Regional brain iron, ferritin and transferrin concentrations during iron deficiency and iron repletion in developing rats, *J. Nutr.* 127 (1997) 2030–2038.
- [38] D.B. Drachman, K. Frank, M. Dykes-Hoberg, P. Teismann, G. Almer, S. Przedborski, J.D. Rothstein, Cyclooxygenase 2 inhibition protects motor neurons and prolongs survival in a transgenic mouse model of ALS, *Ann. Neurol.* 52 (2002) 771–778.
- [39] T. Arai, M. Hasegawa, H. Akiyama, K. Ikeda, T. Nonaka, H. Mori, D. Mann, K. Tsuchiya, M. Yoshida, Y. Hashizume, T. Oda, TDP-43 is a component of ubiquitin-positive tau-negative inclusions in frontotemporal lobar degeneration and amyotrophic lateral sclerosis, *Biochem. Biophys. Res. Commun.* 351 (2006) 602–611.
- [40] I.R. Mackenzie, E.H. Bigio, P.G. Ince, F. Geser, M. Neumann, N.J. Cairns, L.K. Kwong, M.S. Forman, J. Ravits, H. Stewart, A. Eisen, L. McClusky, H.A. Kretschmar, C.M. Monoranu, J.R. Highley, J. Kirby, T. Siddique, P.J. Shaw, V.M. Lee, J.Q. Trojanowski, Pathological TDP-43 distinguishes sporadic amyotrophic lateral sclerosis from amyotrophic lateral sclerosis with SOD1 mutations, *Ann. Neurol.* 61 (2007) 427–434.
- [41] J. Robertson, T. Sanelli, S. Xiao, W. Yang, P. Horne, R. Hammond, E.P. Piore, M.J. Strong, Lack of TDP-43 abnormalities in mutant SOD1 transgenic mice shows disparity with ALS, *Neurosci. Lett.* 420 (2007) 128–132.
- [42] C.F. Tan, H. Eguchi, A. Tagawa, O. Onodera, T. Iwasaki, A. Tsujino, M. Nishizawa, A. Kakita, H. Takahashi, TDP-43 immunoreactivity in neuronal inclusions in familial amyotrophic lateral sclerosis with or without SOD1 gene mutation, *Acta Neuropathol.* 113 (2007) 535–542.
- [43] X.W. Su, S.Y. Lee, R.M. Mitchell, H.E. Stephens, Z. Simmons, J.R. Connor, H63D HFE polymorphisms are associated with increased disease duration and decreased muscle superoxide dismutase-1 expression in amyotrophic lateral sclerosis patients, *Muscle Nerve* 48 (2013) 242–246.
- [44] T.D. Heiman-Patterson, J.S. Deitch, E.P. Blankenhorn, K.L. Erwin, M.J. Perreault, B.K. Alexander, N. Byers, I. Toman, G.M. Alexander, Background and gender effects on survival in the TgN(SOD1-G93A)1Gur mouse model of ALS, *J. Neurol. Sci.* 236 (2005) 1–7.
- [45] T.D. Heiman-Patterson, R.B. Sher, E.A. Blankenhorn, G. Alexander, J.S. Deitch, C.B. Kunst, N. Maragakis, G. Cox, Effect of genetic background on phenotype variability in transgenic mouse models of amyotrophic lateral sclerosis: a window of opportunity in the search for genetic modifiers, *Amyotroph. Lateral Scler.* 12 (2011) 79–86.

- [46] R. Mancuso, S. Olivan, P. Mancera, A. Pasten-Zamorano, R. Manzano, C. Casas, R. Osta, X. Navarro, Effect of genetic background on onset and disease progression in the SOD1-G93A model of amyotrophic lateral sclerosis, *Amyotroph. Lateral Scler.* 13 (2012) 302–310.
- [47] T. Moos, Immunohistochemical localization of intraneuronal transferrin receptor immunoreactivity in the adult mouse central nervous system, *J. Comp. Neurol.* 375 (1996) 675–692.
- [48] T.K. Dickinson, J.R. Connor, Immunohistochemical analysis of transferrin receptor: regional and cellular distribution in the hypotransferrinemic (hpx) mouse brain, *Brain Res.* 801 (1998) 171–181.
- [49] T. Moos, P.S. Oates, E.H. Morgan, Expression of the neuronal transferrin receptor is age dependent and susceptible to iron deficiency, *J. Comp. Neurol.* 398 (1998) 420–430.
- [50] L. Zecca, M.B. Youdim, P. Riederer, J.R. Connor, R.R. Crichton, Iron, brain ageing and neurodegenerative disorders, *Nat. Rev. Neurosci.* 5 (2004) 863–873.
- [51] J.R. Connor, K.L. Boeshore, S.A. Benkovic, S.L. Menzies, Isoforms of ferritin have a specific cellular distribution in the brain, *J. Neurosci. Res.* 37 (1994) 461–465.
- [52] K.I. Rathore, A. Redensek, S. David, Iron homeostasis in astrocytes and microglia is differentially regulated by TNF-alpha and TGF-beta1, *Glia* 60 (2012) 738–750.
- [53] S.H. Appel, W. Zhao, D.R. Beers, J.S. Henkel, The microglial–motoneuron dialogue in ALS, *Acta Myol.* 30 (2011) 4–8.
- [54] R.M. Mitchell, Z. Simmons, J.L. Beard, H.E. Stephens, J.R. Connor, Plasma biomarkers associated with ALS and their relationship to iron homeostasis, *Muscle Nerve* 42 (2010) 95–103.
- [55] M.A. Burguillos, T. Deierborg, E. Kavanagh, A. Persson, N. Hajji, A. Garcia-Quintanilla, J. Cano, P. Brundin, E. Englund, J.L. Venero, B. Joseph, Caspase signalling controls microglia activation and neurotoxicity, *Nature* 472 (2011) 319–324.
- [56] S. Boillee, K. Yamanaka, C.S. Lobsiger, N.G. Copeland, N.A. Jenkins, G. Kassiotis, G. Kollias, D.W. Cleveland, Onset and progression in inherited ALS determined by motor neurons and microglia, *Science* 312 (2006) 1389–1392.
- [57] K. Yamanaka, S.J. Chun, S. Boillee, N. Fujimori-Tonou, H. Yamashita, D.H. Gutmann, R. Takahashi, H. Misawa, D.W. Cleveland, Astrocytes as determinants of disease progression in inherited amyotrophic lateral sclerosis, *Nat. Neurosci.* 11 (2008) 251–253.
- [58] M. Nagai, D.B. Re, T. Nagata, A. Chalazonitis, T.M. Jessell, H. Wichterle, S. Przedborski, Astrocytes expressing ALS-linked mutated SOD1 release factors selectively toxic to motor neurons, *Nat. Neurosci.* 10 (2007) 615–622.
- [59] S.H. Lee, J.W. Kim, S.H. Shin, K.P. Kang, H.C. Choi, S.H. Choi, K.U. Park, H.Y. Kim, W. Kang, S.H. Jeong, HFE gene mutations, serum ferritin level, transferrin saturation, and their clinical correlates in a Korean population, *Dig. Dis. Sci.* 54 (2009) 879–886.
- [60] S. Petri, S. Korner, M. Kiaei, Nrf2/ARE signaling pathway: key mediator in oxidative stress and potential therapeutic target in ALS, *Neurol. Res. Int.* 2012 (2012) 878030.
- [61] A. Sarlette, K. Krampfl, C. Grothe, N. Neuhoff, R. Dengler, S. Petri, Nuclear erythroid 2-related factor 2-antioxidative response element signaling pathway in motor cortex and spinal cord in amyotrophic lateral sclerosis, *J. Neuropathol. Exp. Neurol.* 67 (2008) 1055–1062.
- [62] M. Pehar, M.R. Vargas, K.M. Robinson, P. Cassina, P.J. Diaz-Amarilla, T.M. Hagen, R. Radi, L. Barbeito, J.S. Beckman, Mitochondrial superoxide production and nuclear factor erythroid 2-related factor 2 activation in p75 neurotrophin receptor-induced motor neuron apoptosis, *J. Neurosci.* 27 (2007) 7777–7785.
- [63] A. Neymotin, N.Y. Calingasan, E. Wille, N. Naseri, S. Petri, M. Damiano, K.T. Liby, R. Risingsong, M. Sporn, M.F. Beal, M. Kiaei, Neuroprotective effect of Nrf2/ARE activators, CDDO ethylamide and CDDO trifluoroethylamide, in a mouse model of amyotrophic lateral sclerosis, *Free Radic. Biol. Med.* 51 (2011) 88–96.
- [64] T.W. Kensler, N. Wakabayashi, S. Biswal, Cell survival responses to environmental stresses via the Keap1–Nrf2–ARE pathway, *Annu. Rev. Pharmacol. Toxicol.* 47 (2007) 89–116.
- [65] M.R. Vargas, D.A. Johnson, J.A. Johnson, Decreased glutathione accelerates neurological deficit and mitochondrial pathology in familial ALS-linked hSOD1(G93A) mice model, *Neurobiol. Dis.* 43 (2011) 543–551.
- [66] H. Sumi, S. Kato, Y. Mochimaru, H. Fujimura, M. Etoh, S. Sakoda, Nuclear TAR DNA binding protein 43 expression in spinal cord neurons correlates with the clinical course in amyotrophic lateral sclerosis, *J. Neuropathol. Exp. Neurol.* 68 (2009) 37–47.
- [67] M.E. Gurney, H. Pu, A.Y. Chiu, M.C. Dal Canto, C.Y. Polchow, D.D. Alexander, J. Caliendo, A. Hentati, Y.W. Kwon, H.X. Deng, et al., Motor neuron degeneration in mice that express a human Cu, Zn superoxide dismutase mutation, *Science* 264 (1994) 1772–1775.
- [68] J.P. Julien, A role for neurofilaments in the pathogenesis of amyotrophic lateral sclerosis, *Biochem. Cell Biol. (Biochim. Biol. Cell.)*, 73 (1995) 593–597.
- [69] D.A. Figlewicz, A. Krizus, M.G. Martinoli, V. Meisinger, M. Dib, G.A. Rouleau, J.P. Julien, Variants of the heavy neurofilament subunit are associated with the development of amyotrophic lateral sclerosis, *Hum. Mol. Genet.* 3 (1994) 1757–1761.
- [70] J. Brettschneider, A. Petzold, S.D. Sussmuth, A.C. Ludolph, H. Tümani, Axonal damage markers in cerebrospinal fluid are increased in ALS, *Neurology* 66 (2006) 852–856.
- [71] T.S. Reijn, W.F. Abdo, H.J. Schelhaas, M.M. Verbeek, CSF neurofilament protein analysis in the differential diagnosis of ALS, *J. Neurol.* 256 (2009) 615–619.
- [72] J. Ganesalingam, J. An, R. Bowser, P.M. Andersen, C.E. Shaw, pNFH is a promising biomarker for ALS, *Amyotroph. Lateral Scler. Frontotemporal Degener.* 14 (2013) 146–149.
- [73] K. Boylan, C. Yang, J. Crook, K. Overstreet, M. Heckman, Y. Wang, D. Borchelt, G. Shaw, Immunoreactivity of the phosphorylated axonal neurofilament H subunit (pNF-H) in blood of ALS model rodents and ALS patients: evaluation of blood pNF-H as a potential ALS biomarker, *J. Neurochem.* 111 (2009) 1182–1191.
- [74] L.E. Rosengren, J.E. Karlsson, J.O. Karlsson, L.I. Persson, C. Wikkelso, Patients with amyotrophic lateral sclerosis and other neurodegenerative diseases have increased levels of neurofilament protein in CSF, *J. Neurochem.* 67 (1996) 2013–2018.
- [75] H. Zetterberg, J. Jacobsson, L. Rosengren, K. Blennow, P.M. Andersen, Cerebrospinal fluid neurofilament light levels in amyotrophic lateral sclerosis: impact of SOD1 genotype, *Eur. J. Neurol.* 14 (2007) 1329–1333.